



Laboratori Nazionali del Gran Sasso

5 giugno 2024



A test of Local Lorentz Invariance with the LAGEOS II satellite

David Lucchesi

Istituto di Astrofisica e Planetologia Spaziali (IAPS) – Istituto Nazionale di Astrofisica (INAF)

Via Fosso del Cavaliere n. 100, 00133 Tor Vergata, Roma

Istituto Nazionale di Fisica Nucleare (INFN)

Via della Ricerca Scientifica n. 1, 00133 Tor Vergata, Roma

david.lucchesi@inaf.it





Summary

- The LARASE and SaToR-G experiments
- SLR, POD and Models
- Local Lorentz Invariance
- Conclusions





The LARASE and SaToR-G experiments

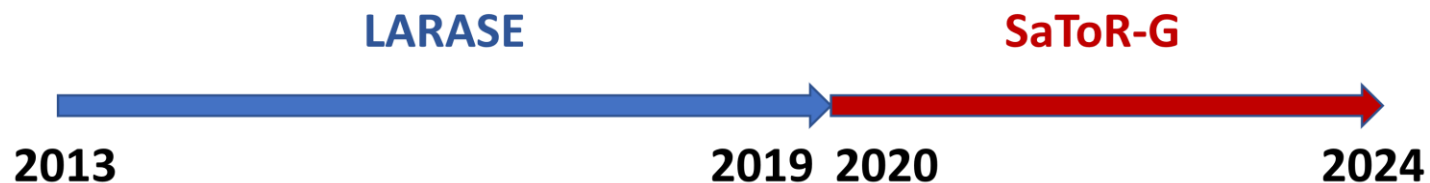


The **LA**ser **RA**nged **Sa**ttellites **E**xperiment (**LARASE**, 2013-2019) and **Sa**ttellite **T**ests **o**f **R**elativistic **G**ravity (**SaToR-G**, started on 2020) are two experiments devoted to measurements of the gravitational interaction in the **Weak-Field** and **Slow-Motion (WFSM)** limit of **General Relativity (GR)** by means of laser tracking to geodetic passive satellites orbiting around the Earth. The two experiments were and are funded by the **Italian National Institute for Nuclear Physics (INFN-CSN2)**.

In particular, **SaToR-G** aims to test gravitation beyond the predictions of **Einstein's Theory of GR** searching for effects foreseen by **alternative theories of gravitation (ATG)** and possibly connected with *'new physics'*.

SaToR-G builds on the improved dynamical model of the two **LAGEOS** and **LARES** satellites achieved within the previous project **LARASE**.

The improvements concern the modeling of both **gravitational** and **non-gravitational perturbations**.





The LARASE and SaToR-G experiments



From the analysis of **satellite orbits** it is possible to obtain a series of measurements of **gravitational effects** with consequent constraints on **different theories of gravitation**. The main measures include:

1. **Relativistic precessions**
2. **Constraints on long-range interactions**
3. **Nonlinearity of the gravitational interaction**
4. **Local Lorentz Invariance**
5. **Equivalence Principle**
6. ...

From these measurements it is possible to obtain **constraints** on the **parametrized post-Newtonian (PPN) parameters** and their combinations.

The ultimate goal is to provide **precise** and **accurate measures**, in the sense of a **robust** and **reliable evaluation** of **systematic errors**, in order to obtain **significant constraints** for the **different theories**.



The LARASE and SaToR-G experiments



Weak Equivalence Principle (WEP)

- two different bodies fall with the same acceleration: Universality of the Free Fall (**UFF**)
- the inertial mass is proportional to the gravitational (passive) mass
- the trajectory of a freely falling “test” body is independent of its internal structure and composition
- in every local and non-rotating falling frame, the trajectory of a freely falling test body is a straight line, in agreement with special relativity

Einstein Equivalence Principle (EEP)

- **WEP**
- Local Lorentz Invariance (**LLI**)
 - The outcome of any local non-gravitational experiment is independent of the velocity of the freely-falling reference frame in which it is performed
- Local Position Invariance (**LPI**)
 - The outcome of any local non-gravitational experiment is independent of where and when in the universe it is performed

Metric theories

- GR is a metric theory of gravitation and all metric theories obey the EEP
- Indeed, the experimental results supporting the EEP supports the conclusion that the only theories of gravity that have a hope of being viable are metric theories, or possibly theories that are metric apart from very weak or short-range non-metric couplings (as in string theory):

1. there exist a symmetric metric
2. tests masses follow geodesics of the metric
3. in Local Lorentz Frames, the non-gravitational laws of physics are those of Special Relativity

$$g_{\alpha\beta} = g_{\beta\alpha}$$

$$\det(g_{\alpha\beta}) \neq 0$$

$$ds^2 = g_{\alpha\beta} dx^\alpha dx^\beta$$

$$G_{\alpha\beta} = 8\pi \frac{G}{c^4} T_{\alpha\beta}$$

$$G_{\alpha\beta} = R_{\alpha\beta} - \frac{1}{2} R g_{\alpha\beta} + \Lambda g_{\alpha\beta}$$



The LARASE and SaToR-G experiments



The parametrized post-Newtonian (PPN) formalism

- Post-Newtonian formalism or **PPN** formalism details the parameters in which different metric theories of gravity, under **WFSM** conditions, can differ from Newtonian gravity.

Nordtvedt, K. *Equivalence Principle for Massive Bodies. II. Theory*. Phys. Rev. **1968**, 169, 1017–1025

Will, C.M. *Theoretical Frameworks for Testing Relativistic Gravity. II. Parametrized Post-Newtonian Hydrodynamics, and the Nordtvedt Effect*. Astrophys. J. **1971**, 163, 611–628

Will, C.M.; Nordtvedt, K. *Conservation Laws and Preferred Frames in Relativistic Gravity. I. Preferred-Frame Theories and an Extended PPN Formalism*. Astrophys. J. **1972**, 177, 757–774

Consequently, the natural theoretical framework to test gravitation will be that of the **Parameterized Post-Newtonian (PPN)** formalism.

However, we also try to apply, as far as possible, the approach suggested by **R. H. Dicke** more than 50 years ago, usually referred to as the **Dicke framework**:

- this is a fairly general framework that allows us to conceive experiments not connected, *a priori*, with a given physical theory and also provides a way to analyze the results of an experiment under primary hypotheses.

Dicke, R.H. *The Theoretical Significance of Experimental Relativity*; Blackie and Son Ltd.: London/Glasgow, UK, **1964**

The parametrized post-Newtonian (PPN) formalism

- One way to test a theory of gravitation is by studying its post-Newtonian limit
- Post-Newtonian formalism or **PPN** formalism details the parameters in which different metric theories of gravity, under **WFSM** conditions, can differ from Newtonian gravity

C.M. Will *Living Rev. Relativity*, 17, (2014), 4

$$g_{00} = -1 + 2U - 2\beta U^2 - 2\xi\Phi_W + (2\gamma + 2 + \alpha_3 + \zeta_1 - 2\xi)\Phi_1 + 2(3\gamma - 2\beta + 1 + \zeta_2 + \xi)\Phi_2 + 2(1 + \zeta_3)\Phi_3 + 2(3\gamma + 3\zeta_4 - 2\xi)\Phi_4 - (\zeta_1 - 2\xi)\mathcal{A} - (\alpha_1 - \alpha_2 - \alpha_3)w^2U - \alpha_2 w^i w^j U_{ij} + (2\alpha_3 - \alpha_1)w^i V_i + \mathcal{O}(\epsilon^3),$$

$$g_{0i} = -\frac{1}{2}(4\gamma + 3 + \alpha_1 - \alpha_2 + \zeta_1 - 2\xi)V_i - \frac{1}{2}(1 + \alpha_2 - \zeta_1 + 2\xi)W_i - \frac{1}{2}(\alpha_1 - 2\alpha_2)w^i U - \alpha_2 w^j U_{ij} + \mathcal{O}(\epsilon^{5/2}),$$

$$g_{ij} = (1 + 2\gamma U)\delta_{ij} + \mathcal{O}(\epsilon^2).$$

Metric

$$T^{00} = \rho(1 + \Pi + v^2 + 2U),$$

$$T^{0i} = \rho v^i \left(1 + \Pi + v^2 + 2U + \frac{p}{\rho} \right),$$

$$T^{ij} = \rho v^i v^j \left(1 + \Pi + v^2 + 2U + \frac{p}{\rho} \right) + p\delta^{ij}(1 - 2\gamma U).$$

Stress-Energy Tensor

$$U = \int \frac{\rho'}{|\mathbf{x} - \mathbf{x}'|} d^3 x',$$

$$U_{ij} = \int \frac{\rho'(x - x')_i (x - x')_j}{|\mathbf{x} - \mathbf{x}'|^3} d^3 x',$$

$$\Phi_W = \int \frac{\rho' \rho'' (\mathbf{x} - \mathbf{x}')}{|\mathbf{x} - \mathbf{x}'|^3} \cdot \left(\frac{\mathbf{x}' - \mathbf{x}''}{|\mathbf{x} - \mathbf{x}''|} - \frac{\mathbf{x} - \mathbf{x}''}{|\mathbf{x}' - \mathbf{x}''|} \right) d^3 x' d^3 x'',$$

$$\mathcal{A} = \int \frac{\rho' [\mathbf{v}' \cdot (\mathbf{x} - \mathbf{x}')]^2}{|\mathbf{x} - \mathbf{x}'|^3} d^3 x',$$

$$\Phi_1 = \int \frac{\rho' v'^2}{|\mathbf{x} - \mathbf{x}'|} d^3 x',$$

$$\Phi_2 = \int \frac{\rho' U'}{|\mathbf{x} - \mathbf{x}'|} d^3 x',$$

$$\Phi_3 = \int \frac{\rho' \Pi'}{|\mathbf{x} - \mathbf{x}'|} d^3 x',$$

$$\Phi_4 = \int \frac{p'}{|\mathbf{x} - \mathbf{x}'|} d^3 x',$$

$$V_i = \int \frac{\rho' v'_i}{|\mathbf{x} - \mathbf{x}'|} d^3 x',$$

$$W_i = \int \frac{\rho' [\mathbf{v}' \cdot (\mathbf{x} - \mathbf{x}')] (x - x')_i}{|\mathbf{x} - \mathbf{x}'|^3} d^3 x'.$$

Metric Potentials



The LARASE and SaToR-G experiments



In 1971, **Thorne** and **Will** remarked that:

- “ . . . It is important for the future that experimenters concentrate not only on measuring the **PPN** parameters. They should also perform new experiments within the **Dicke framework** to strengthen—or destroy—the foundation it lays for the **PPN framework** . . . ”

Thorne, K.S.; Will, C.M. Theoretical Frameworks for Testing Relativistic Gravity. I. Foundations. *Astrophys. J.* **1971**, 163, 595

We analyzed these aspects in more detail in 2021 in the paper introducing the **SaToR-G** experiment:

D. Lucchesi, L. Anselmo, M. Bassan, et al., *Testing Gravitational Theories in the Field of the Earth with the SaToR-G Experiment*. *Universe* 7, 192, <https://doi.org/10.3390/universe7060192>, **2021**

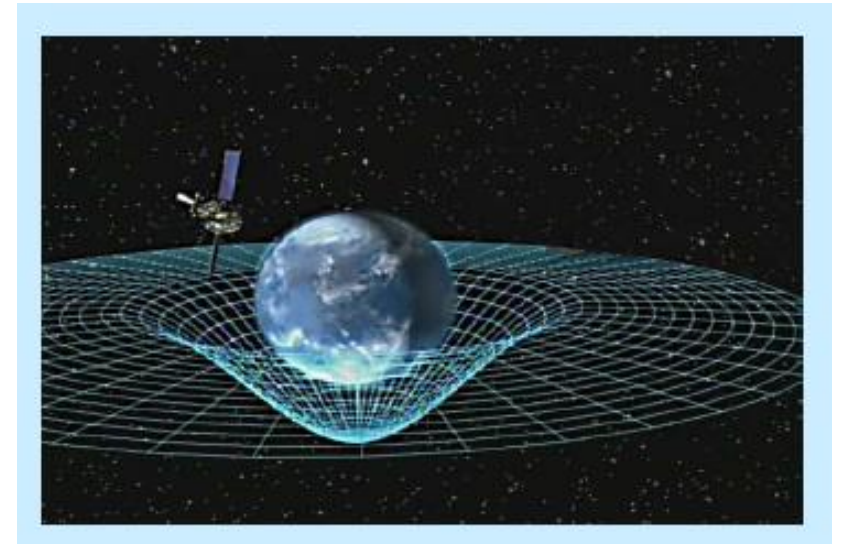
Gravity theories different from **GR** provide additional fields beside the metric tensor $g_{\alpha\beta}$, that act as “new” gravitational fields:

- **Scalar**
- **Vector**
- **Tensor**

The role of these gravitational fields is to “mediate” how the matter and the non-gravitational fields generate the gravitational fields and produce the metric.

In Metric theories different from GR

- spacetime geometry tells mass-energy how to move as in **GR**
- but mass-energy tells spacetime geometry how to curve in a different way from **GR**
- the metric alone acts back on the mass in agreement with **EEP** as in **GR**.



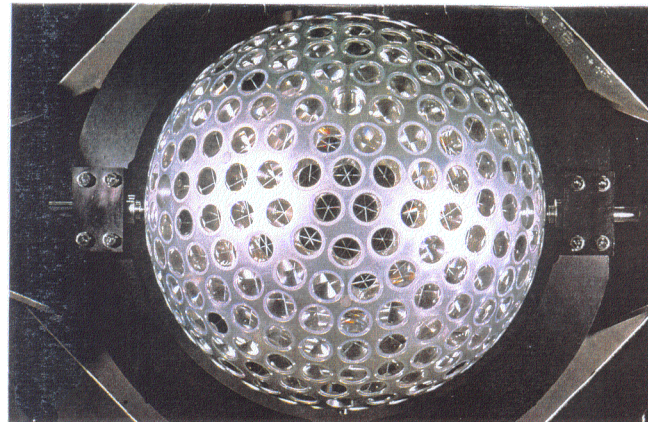
The LARASE and SaToR-G experiments

The predictions of **GR** on the orbits of **geodetic satellites**, which play the role of **test masses**, will be compared with those of **ATG** both metric and non-metric in their essence.

Parameter	Unit	Symbol	LAGEOS	LAGEOS II	LARES
Semi-major axis	km	a	12 270.00	12 162.08	7 820.31
Eccentricity	-	e	0.0044	0.0138	0.0012
Inclination	deg.	i	109.84	52.66	69.49
Radius	cm	R	30.0	30.0	18.2
Mass	kg	M	406.9	405.4	383.8
Area/Mass	m ² /kg	A/M	6.94×10 ⁻⁴	6.97×10 ⁻⁴	2.69×10 ⁻⁴



LAGEOS (NASA, 1976)



LAGEOS II (ASI/NASA, 1992)



LARES (ASI, 2012)

SLR, POD and Models

The **geodetic** satellites are tracked with very high accuracy through the powerful **Satellite Laser Ranging (SLR)** technique.

The **SLR** represents a very impressive and powerful technique to determine the **round-trip time** between **Earth-bound laser Stations** and **orbiting passive** (and not **passive**) **satellites**.

The time series of range measurements are then a record of the motions of both the end points: the Satellite and the Station.

Thanks to the accurate modelling of both **gravitational** and **non-gravitational perturbations** on the orbit of these satellites — less than 1 cm in **range accuracy** — we are able to determine their **Keplerian elements** with about the same **accuracy**.

The precision of the measurement depends mainly from the laser pulse width, about $1 \cdot 10^{-10}$ s — $3 \cdot 10^{-11}$ s

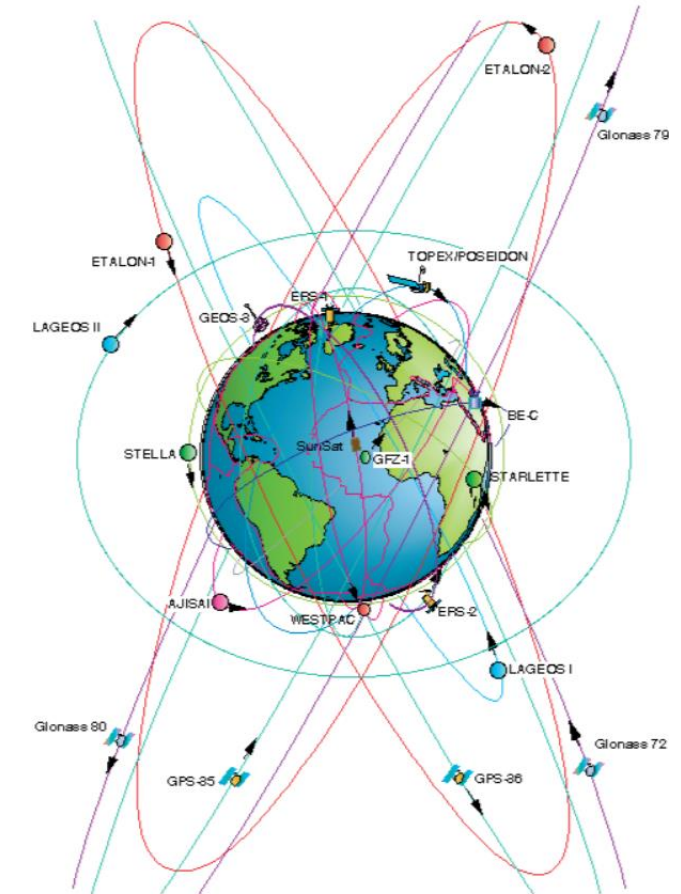
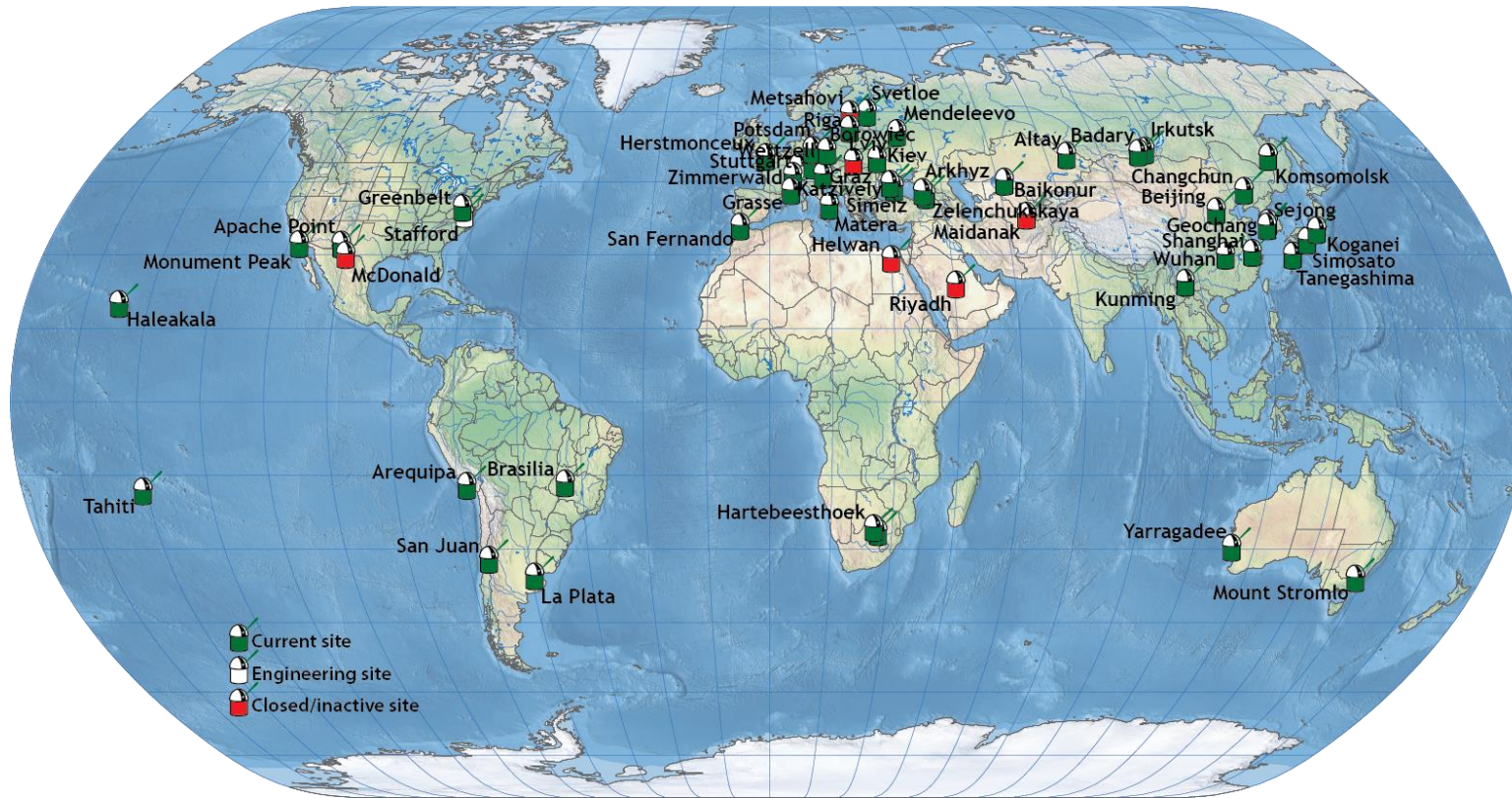
Matera (ASI-CGS)



SLR, POD and Models

The **ILRS (International Laser Ranging Service)** supports laser ranging measurements to **geodetic**, **remote sensing**, **navigation**, and **experimental satellites** equipped with retroreflector arrays as well as to **reflectors on the Moon**.

ilrs.gsfc.nasa.gov



SLR, POD and Models



Precise Orbit Determination (POD) has the **goal** of accurately determining the **position** and **velocity vectors** of an orbiting satellite.

To achieve this objective, **precise observations** of the satellite's **motion** and a **dynamic model** of the orbit as **accurate** as possible are necessary.

With these two ingredients it is possible to compute the **observable** to be **minimized** in a **least squares process**.

In the case of **SLR**, this **observable** is a **quadratic function** of the **range residuals R** :

$$\mathcal{R}_i = O_i - C_i$$

Orbits:

$$\frac{d}{dt} \vec{x} = f(\vec{x}, t, \vec{\alpha}) \quad \text{Differential equation}$$

$$\begin{cases} \vec{x} \in \mathbb{R}^\ell \\ \vec{\alpha} \in \mathbb{R}^m \end{cases} \quad \begin{array}{l} \text{State vector (position and velocity, ...)} \\ \text{Models dynamic parameters (C}_{20}, C_r, \dots) \end{array}$$

$$\vec{x}(t_0 = \vec{x}_0 \in \mathbb{R}^\ell) \quad \text{Initial condition at a given epoch: } \ell = 6 + \dots$$

$$\vec{x} = \vec{x}(t, \vec{x}_0, \vec{\alpha}) \quad \text{General solution for the orbits (integral flow)}$$

Observations:

$$C = C(\vec{x}, t, \vec{\beta}) \quad \text{Observation function, } \vec{\beta} \in \mathbb{R}^n \quad \text{kinematic parameters}$$

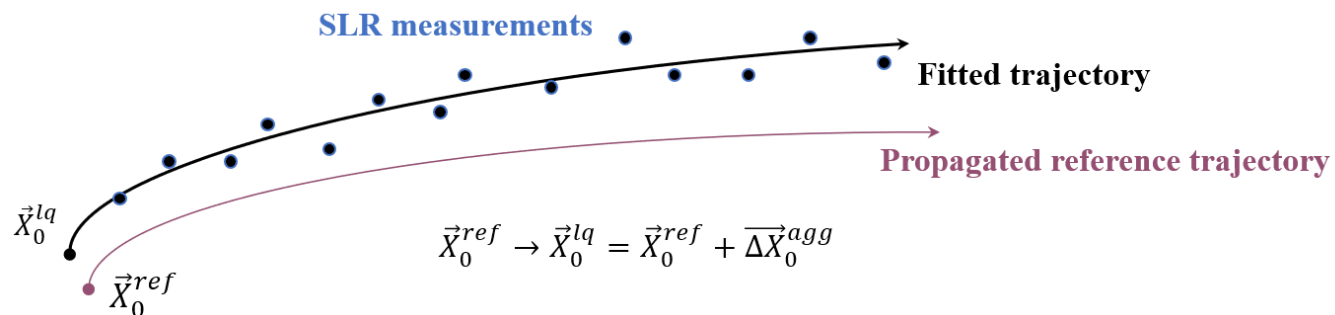
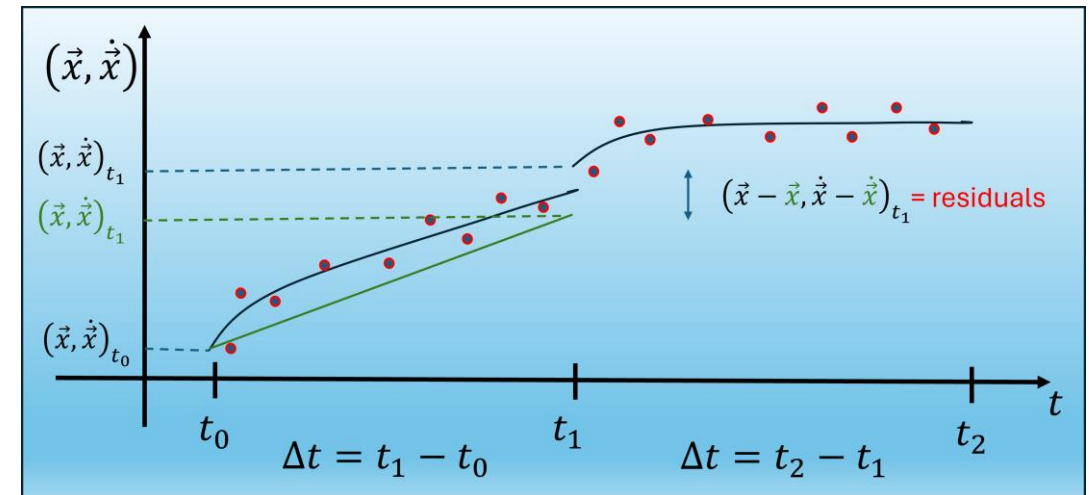
$$R_i = O_i - C_i = O_i - C(\vec{x}(t_i), t_i, \vec{\beta}) = \sum_j \frac{\partial C_i}{\partial P_j} \delta P_j + \delta O_i \quad Q(\vec{R}) = \frac{1}{q} \vec{R}^T \vec{R} = \frac{1}{q} \sum_{i=1}^q R_i^2$$

SLR, POD and Models

Currently, we are using the following software in our **POD**:

- **GEODYN II** (NASA/GSFC)
- **SATAN** (NSGF, UK) in collaboration with “Observatorio de YEBES” (Spain) (**under test**)
- **Bernese** (Univ. Berna, CH)

1. From a least squares fit of the tracking data by means of an appropriate dynamic model, the estimate of the state vector of the satellite over 7-day arcs is obtained.
2. Then from an appropriate comparison between the state vector estimated at the beginning of each arc with the state vector estimated at the beginning of the previous arc but propagated at the same epoch, the residuals in the orbital elements are obtained: $\Delta \vec{x}_{res} = \vec{x}_{est} - \vec{x}_{pro}$



D. Lucchesi, G. Balmino, The LAGEOS satellites orbital residuals determination and the Lense-Thirring effect measurement. Plan. and Space Science, doi:10.1016/j.pss.2006.03.001, 2006

SLR, POD and Models

POD and Models for the two LAGEOS and LARES satellites

GEODYN II s/w

- Arc length, 7 days
- General Relativity: not modeled
- Empirical accelerations, CR, ...: not estimated
- Non-gravitational perturbations: internal and external
- Gravity field: from GRACE and GRACE-FO solutions
- State-vector adjusted to best fit the tracking data
- ...

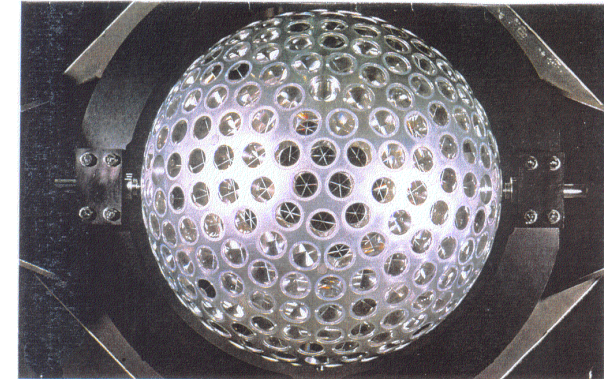


TABLE III. Models currently used for the POD obtained from GEODYN II. The models are grouped in gravitational perturbations, non-gravitational perturbations and reference frames realizations.

Model for	Model type	Reference
Geopotential (static)	EIGEN-GRACE02S/GGM05S	[42–44]
Geopotential (time-varying: even zonal harmonics)	GRACE/GRACE FO	[43, 44]
Geopotential (time-varying: tides)	Ray GOT99.2	[45]
Geopotential (time-varying: non tidal)	IERS Conventions 2010	[41]
Third-body	JPL DE-403	[46]
Relativistic corrections	Parameterized post-Newtonian	[40, 47]
Direct solar radiation pressure	Cannonball	[38]
Earth albedo	Knocke-Rubincam	[48]
Earth-Yarkovsky	Rubincam	[49–51]
Neutral drag	JR-71/MSIS-86	[52, 53]
Spin	LASSOS	[54]
Stations position	ITRF2008/2014	[55, 56]
Ocean loading	Schernek and GOT99.2 tides	[38, 45]
Earth Rotation Parameters	IERS EOP C04	[57]
Nutation	IAU 2000	[58]
Precession	IAU 2000	[59]

SLR, POD and Models



The **dynamic model** aims to reconstruct the **position** and **velocity** of the satellite taking into account three main aspects:

1. **gravitational perturbations**
2. **non-gravitational perturbations**
3. **reference systems.**

We will focus on the first two points:

1. **Gravitational perturbations (GPs)**
2. **Non-gravitational perturbations (NGPs).**

SLR, POD and Models

The **dynamic model** aims to reconstruct the **position** and **velocity** of the satellite taking into account three main aspects:

1. **gravitational perturbations**
2. **non-gravitational perturbations**
3. **reference systems.**

$$\dot{\omega}_{Schw} = \frac{3 (GM_{\oplus})^{3/2}}{c^2 a^{5/2} (1 - e^2)}$$

$$\dot{\omega}_{LT} = -\frac{6G}{c^2 a^3} \frac{J_{\oplus}}{(1 - e^2)^{3/2}} \cos i$$

We will focus on the first two points:

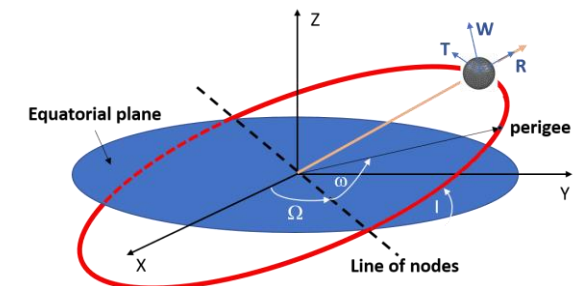
$$\dot{\Omega}_{LT} = \frac{2G}{c^2 a^3} \frac{J_{\oplus}}{(1 - e^2)^{3/2}}$$

1. **Gravitational perturbations (GPs)**
2. **Non-gravitational perturbations (NGPs).**

$$\dot{M}_{Schw} = -\sqrt{1 - e^2} \frac{3 (GM_{\oplus})^{3/2}}{c^2 a^{5/2} (1 - e^2)}$$

In particular we are interested in knowing the effects of these perturbations on some orbital elements, those characterized by **secular effects** produced by **GR**, as:

- **Argument of pericenter, ω**
- **Right ascension of the ascending node, Ω**
- **Mean anomaly, M**



SLR, POD and Models

The GR model for the accelerations

Huang et al., *Celest. Mech. & Dyn. Astron.* 48, 1990

$$\vec{A}_{rel} = \vec{A}_E + \vec{A}_{ds} + \vec{A}_{LT}$$

$$\vec{A}_E = \frac{Gm_{\oplus}}{c^2 r^3} \left[\left(4 \frac{Gm_{\oplus}}{r} - v^2 \right) \vec{r} + 4(\vec{r} * \vec{v})\vec{v} \right]$$

$$\vec{A}_{ds} = 2(\vec{\Omega} \wedge \vec{v})$$

$$\vec{A}_{LT} = 2 \frac{Gm_{\oplus}}{c^2 r^3} \left[\frac{3}{r^2} (\vec{r} \wedge \vec{v})(\vec{r} * \vec{J}) + (\vec{v} \wedge \vec{J}) \right]$$

Relativistic perturbations

Einstein or Schwarzschild component

De Sitter (or geodetic) component

Lense-Thirring component

with:

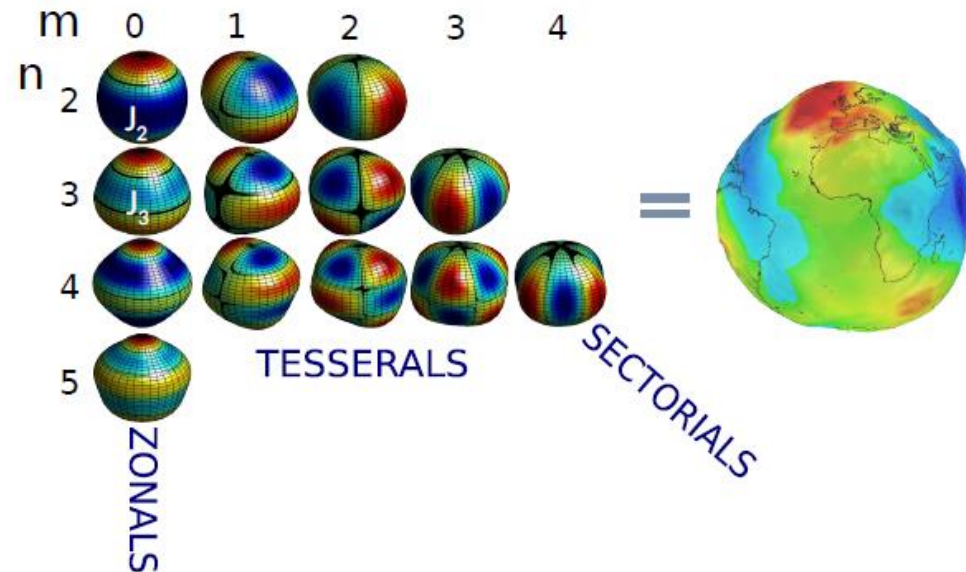
$$\vec{\Omega} \cong \frac{3}{2} (\vec{V}_E - \vec{V}_S) \wedge \left(-\frac{GM_S}{c^2 R_{ES}^3} \right) \vec{X}_{ES}$$

Where, capital letters refer to position, velocity, acceleration and mass in the barycentric reference frame, while small letters refer to the same quantities in the non-inertial geocentric reference system (E=Earth, S=Sun)

SLR, POD and Models

The Earth's potential development in spherical harmonics

$$V(r, \varphi, \lambda) = -\frac{GM_{\oplus}}{r} \left[1 + \sum_{\ell=2}^{\infty} \sum_{m=0}^{\ell} \left(\frac{R_{\oplus}}{r}\right)^{\ell} P_{\ell m}(\sin \varphi) (\bar{C}_{\ell m} \cos m\lambda + \bar{S}_{\ell m} \sin m\lambda) \right]$$



SLR, POD and Models



For instance, the **Einstein-Thirring-Lense** precession is very small compared to the classical precession of the orbit due to the deviation from the spherical symmetry for the distribution of the Earth's mass, or even compared to the same relativistic **Schwarzschild** precession produced by the mass of the primary (≈ 3350 mas/yr for **LAGEOS**)

$$\dot{\Omega}_{LT} = \frac{2G}{c^2 a^3} \frac{J_{\oplus}}{(1 - e^2)^{3/2}}$$

$$V(r, \varphi, \lambda) = -\frac{GM_{\oplus}}{r} \left[1 + \sum_{\ell=2}^{\infty} \sum_{m=0}^{\ell} \left(\frac{R_{\oplus}}{r}\right)^{\ell} P_{\ell m}(\sin \varphi) (\bar{C}_{\ell m} \cos m\lambda + \bar{S}_{\ell m} \sin m\lambda) \right]$$

Rate (mas/yr)	LAGEOS	LAGEOS II	LARES
$\dot{\Omega}_{LT}$	30.67	31.50	118.48

The even zonal harmonics $\bar{C}_{\ell 0}$ are responsible of a secular effect

$$\langle \dot{\Omega}_{class} \rangle_{sec} = -\frac{3}{2} n \left(\frac{R_{\oplus}}{a}\right)^2 \frac{\cos i}{(1 - e^2)^2} \left\{ -\sqrt{5} \bar{C}_{2,0} + \dots \right\}$$

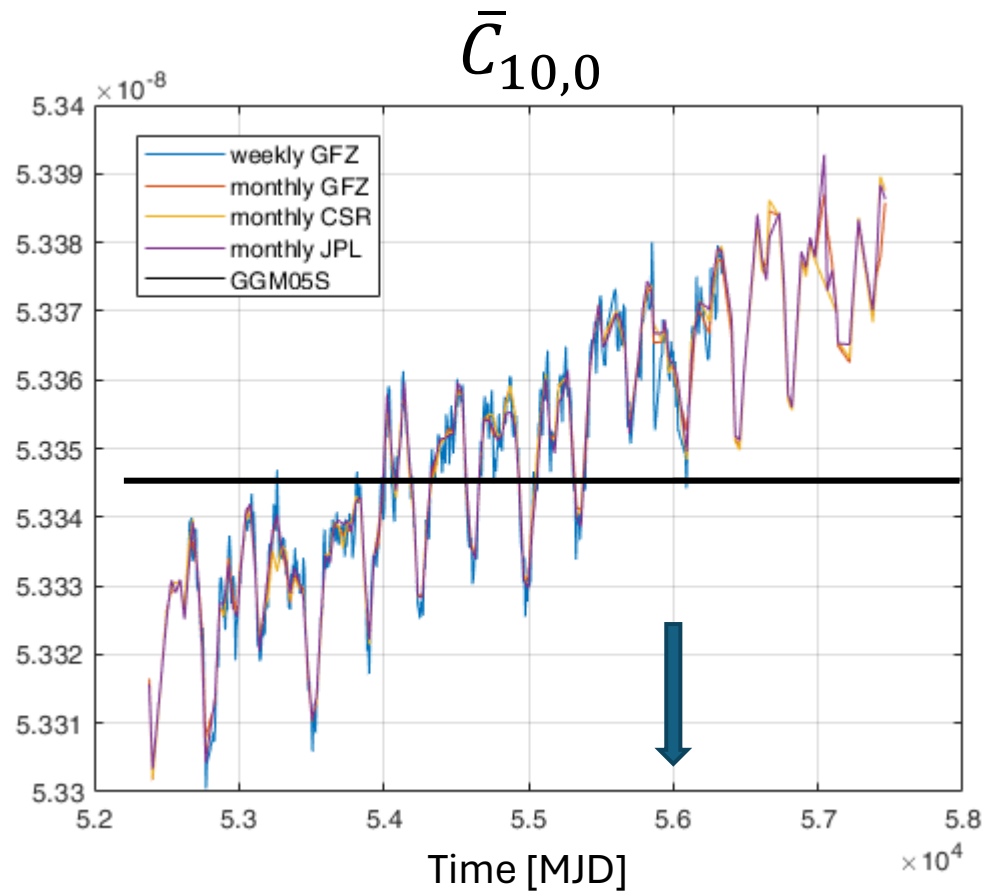
$$\dot{\Omega}_{Lageos}^{Obser} \approx +126 \text{ deg/yr}$$

$$\dot{\Omega}_{LageosII}^{Obser} \approx -231 \text{ deg/yr}$$

$$\dot{\Omega}_{Lares}^{Obser} \approx -624 \text{ deg/yr}$$

SLR, POD and Models

From **GRACE** Temporal Solutions



March 14, 2012

$$V(r, \varphi, \lambda) = -\frac{GM_{\oplus}}{r} \left[1 + \sum_{\ell=2}^{\infty} \sum_{m=0}^{\ell} \left(\frac{R_{\oplus}}{r}\right)^{\ell} P_{\ell m}(\sin \varphi) (\bar{C}_{\ell m} \cos m\lambda + \bar{S}_{\ell m} \sin m\lambda) \right]$$

$$\langle \dot{\Omega}_{class} \rangle_{sec} = -\frac{3}{2} n \left(\frac{R_{\oplus}}{a}\right)^2 \frac{\cos i}{(1-e^2)^2} \left\{ -\sqrt{5} \bar{C}_{2,0} + \dots \right\}$$

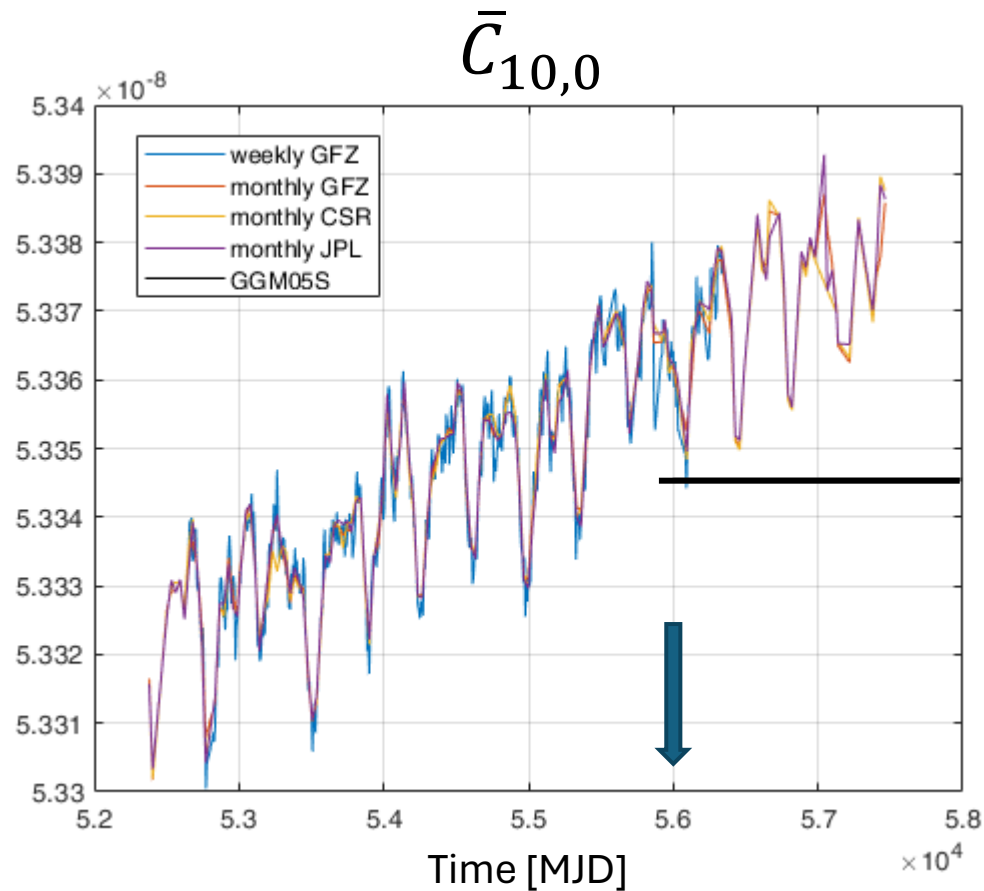
$$\dot{\Omega}_{LT} = \frac{2G}{c^2 a^3} \frac{J_{\oplus}}{(1-e^2)^{3/2}}$$

$$\langle \dot{\omega}_{class} \rangle_{sec} = -\frac{3}{4} n \left(\frac{R_{\oplus}}{a}\right)^2 \frac{1-5\cos^2 i}{(1-e^2)^2} \left\{ -\sqrt{5} \bar{C}_{2,0} + \dots \right\}$$

$$\dot{\omega}_{Schw} = \frac{3(GM_{\oplus})^{3/2}}{c^2 a^{5/2} (1-e^2)} = 3352.58 \text{ mas/yr}$$

SLR, POD and Models

From **GRACE** Temporal Solutions



March 14, 2012

$$V(r, \varphi, \lambda) = -\frac{GM_{\oplus}}{r} \left[1 + \sum_{\ell=2}^{\infty} \sum_{m=0}^{\ell} \left(\frac{R_{\oplus}}{r}\right)^{\ell} P_{\ell m}(\sin \varphi) (\bar{C}_{\ell m} \cos m\lambda + \bar{S}_{\ell m} \sin m\lambda) \right]$$

$$\langle \dot{\Omega}_{class} \rangle_{sec} = -\frac{3}{2} n \left(\frac{R_{\oplus}}{a}\right)^2 \frac{\cos i}{(1-e^2)^2} \left\{ -\sqrt{5} \bar{C}_{2,0} + \dots \right\}$$

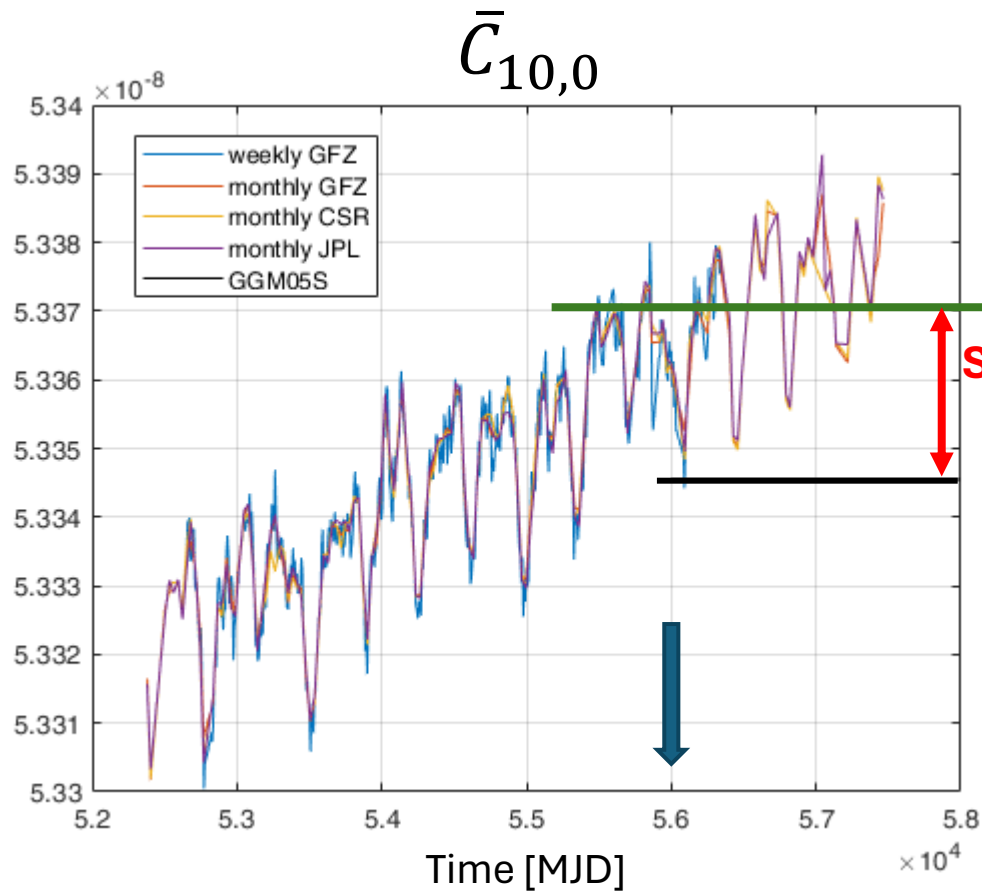
$$\dot{\Omega}_{LT} = \frac{2G}{c^2 a^3} \frac{J_{\oplus}}{(1-e^2)^{3/2}}$$

$$\langle \dot{\omega}_{class} \rangle_{sec} = -\frac{3}{4} n \left(\frac{R_{\oplus}}{a}\right)^2 \frac{1-5\cos^2 i}{(1-e^2)^2} \left\{ -\sqrt{5} \bar{C}_{2,0} + \dots \right\}$$

$$\dot{\omega}_{Schw} = \frac{3(GM_{\oplus})^{3/2}}{c^2 a^{5/2} (1-e^2)} = 3352.58 \text{ mas/yr}$$

SLR, POD and Models

From **GRACE** Temporal Solutions



March 14, 2012

$$V(r, \varphi, \lambda) = -\frac{GM_{\oplus}}{r} \left[1 + \sum_{\ell=2}^{\infty} \sum_{m=0}^{\ell} \left(\frac{R_{\oplus}}{r}\right)^{\ell} P_{\ell m}(\sin \varphi) (\bar{C}_{\ell m} \cos m\lambda + \bar{S}_{\ell m} \sin m\lambda) \right]$$

$$\langle \dot{\Omega}_{class} \rangle_{sec} = -\frac{3}{2} n \left(\frac{R_{\oplus}}{a}\right)^2 \frac{\cos i}{(1-e^2)^2} \left\{ -\sqrt{5} \bar{C}_{2,0} + \dots \right\}$$

$$\dot{\Omega}_{LT} = \frac{2G}{c^2 a^3} \frac{J_{\oplus}}{(1-e^2)^{3/2}}$$

$$\langle \dot{\omega}_{class} \rangle_{sec} = -\frac{3}{4} n \left(\frac{R_{\oplus}}{a}\right)^2 \frac{1-5\cos^2 i}{(1-e^2)^2} \left\{ -\sqrt{5} \bar{C}_{2,0} + \dots \right\}$$

$$\dot{\omega}_{Schw} = \frac{3(GM_{\oplus})^{3/2}}{c^2 a^{5/2} (1-e^2)} = 3352.58 \text{ mas/yr}$$

$$\Delta \bar{C}_{\ell,0} \Rightarrow \Delta \dot{\Omega}_{LT}^{sys} \text{ and } \Delta \dot{\omega}_{LT}^{sys}$$

SLR, POD and Models



In recent years, as part of the previous experiment **LARASE**, we have developed several models to take into account some **perturbations of non-gravitational origin** acting on the **LAGEOS, LAGEOS II** and **LARES** satellites:

- **Spin model**
- **General model for thermal thrust forces due to the Sun and the Earth (to be published)**
- **Neutral drag model**

M. Visco, D. Lucchesi, *Review and critical analysis of mass and moments of inertia of the LAGEOS and LAGEOS II satellites for the LARASE program*. Adv. in Space Res. 57, 044034 doi:10.1016/j.asr.2016.02.006, **2016**

M. Visco, D. Lucchesi, *Comprehensive model for the spin evolution of the LAGEOS and LARES satellites*. Phys. Rev. D 98, 044034 doi:10.1103/PhysRevD.98.044034, **2018**

Pardini, C.; Anselmo, L.; Lucchesi, D.M.; Peron, R., *On the secular decay of the LARES semi-major axis*. Acta Astronautica **2017**, 140, 469–477. doi:10.1016/j.actaastro.2017.09.012

SLR, POD and Models

M. Visco, D. Lucchesi, *Review and critical analysis of mass and moments of inertia of the LAGEOS and LAGEOS II satellites for the LARASE program.* Adv. in Space Res. 57, 044034 doi:10.1016/j.asr.2016.02.006, 2016

Table 1
Materials used for the construction of the two LAGEOS satellites (Cogo, 1988) and their nominal densities.

Satellite	Material density ρ_n (kg/m ³)		
	Hemispheres	Core	Stud
LAGEOS	AA6061 2700 ^a	QQ-B-626 COMP.11 8440 ^a	Cu-Be 8230 ^b
LAGEOS II	AlMgSiCu UNI 6170 2740 ^c	PCuZn39Pb2 UNI 5706 8280 ^c	Cu-Be QQ-C-172 8250 ^c

^a ASM International Handbook Committee (1990).

^b Bauccio (1993).

^c It is the value calculated in Cogo (1988) starting from the measured averaged composition.

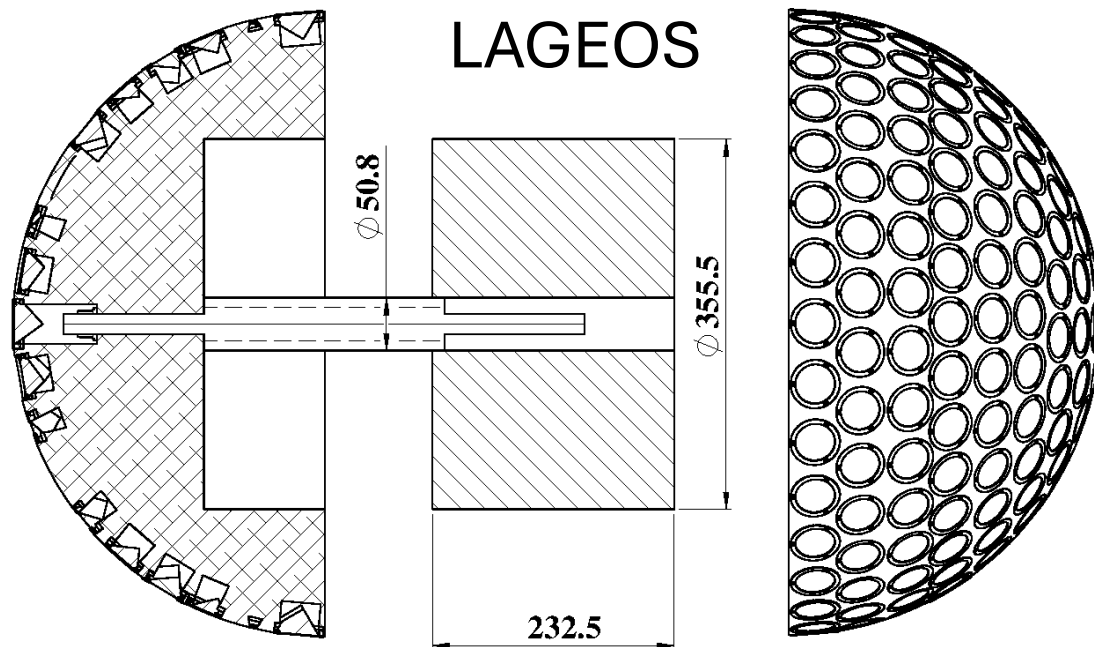
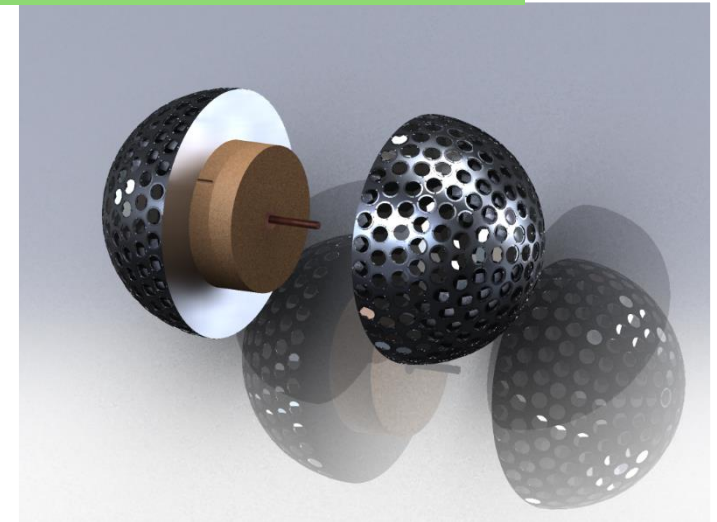


Table 1. Principal moments of inertia of LAGEOS, LAGEOS II and LARES in their flight arrangement.

Satellite	Moments of Inertia (kg m ²)		
	I_{zz}	I_{xx}	I_{yy}
LAGEOS	11.42 ± 0.03	10.96 ± 0.03	10.96 ± 0.03
LAGEOS II	11.45 ± 0.03	11.00 ± 0.03	11.00 ± 0.03
LARES	4.77 ± 0.03	4.77 ± 0.03	4.77 ± 0.03

- The two **LAGEOS** have almost the same oblateness of about 0.04
- **LARES** is practically spherical in shape, even if an oblateness as small as 0.002 is however possible

SLR, POD and Models



M. Visco, D. Lucchesi, *Review and critical analysis of mass and moments of inertia of the LAGEOS and LAGEOS II satellites for the LARASE program*. Adv. in Space Res. 57, 044034 doi:10.1016/j.asr.2016.02.006, 2016

Documents on LAGEOS

- NASA, 1975. LAGEOS Phase B Technical Report, NASA Technical Memorandum X-64915. Technical Report TMX-64915. Marshall Space Flight Center. Marshall Space Flight Center, Alabama 35812. February 1975
- Siry, J.W., 1975. The LAGEOS system. Technical Report TM-X-73072. NASA
- LAGEOS Press Kit, 1976. NASA (1976) Project LAGEOS Press Kit release 76/67. Technical Report 76/67. NASA. National Aeronautics and Space Administration, Washington, DC
- Fitzmaurice, M.W., Minott, P.O., Abshire, J.B., Rowe, H.E., 1977. Prelaunch Testing of the Laser Geodynamic Satellite. Technical Report TP-1062. NASA
- Wong, C., 1978. Watching the Earth move from space. Sky Telesc., 198–202

Documents on LAGEOS II

- Cogo, F., 1988. Weight discrepancy analysis between LAGEOS 1 and LAGEOS 2 satellites. Technical Report LG-TN-AI-035. Aeritalia
- Fontana, F., 1989. Physical properties of LAGEOS II satellite. Technical Report LG-TN-AI-037. Aeritalia
- Fontana, F., 1990. Physical properties of LAGEOS II satellite. Technical Report LG-TN-AI-037. Aeritalia
- Minott, P.O., Zagwodzki, T.W., Varghese, T., Seldon, M., 1993. Prelaunch Optical Characterization of the Laser Geodynamic Satellite (LAGEOS 2). Technical Report 3400. NASA Technical Paper 3400. National Aeronautics and Space Administration, Washington, DC

SLR, POD and Models



M. Visco, D. Lucchesi, *Comprehensive model for the spin evolution of the LAGEOS and LARES satellites*. Phys. Rev. D 98, 044034
doi:10.1103/PhysRevD.98.044034, 2018

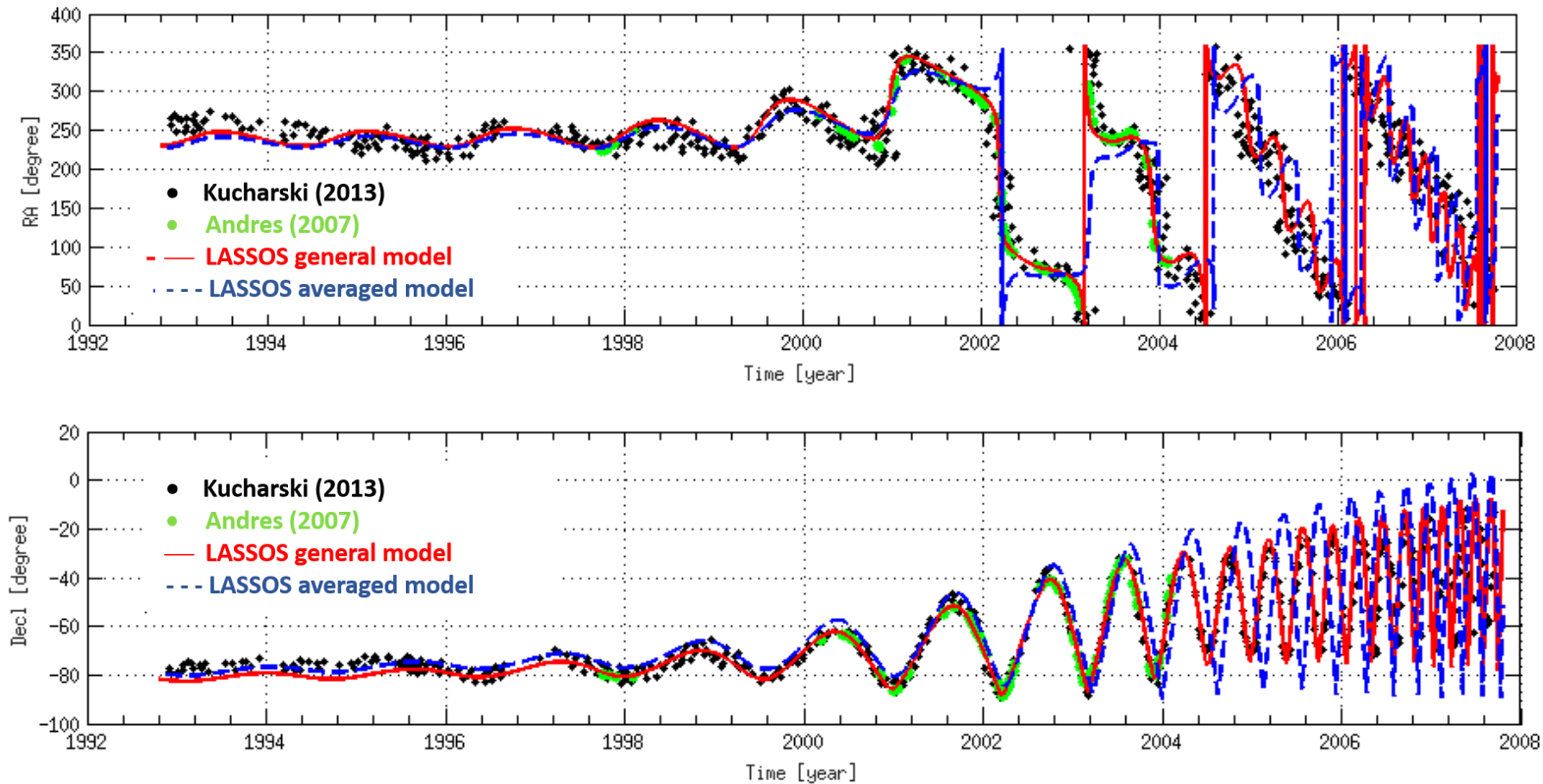
LASSOS Spin Model: results for LAGEOS II

Blue = LASSOS model for the rapid-spin
Red = LASSOS general model

LArase Satellites Spin mOdel Solutions (LASSOS)

Spin Orientation: α , δ

Andrés de la Fuente, J.I.,
2007. *Enhanced Modelling of LAGEOS Non-Gravitational Perturbations* (Ph.D. thesis). Delft University Press. Sieca Repro, Turbineweg 20, 2627 BP Delft, The Netherlands.
Kucharski, D., Lim, H.C., Kirchner, G., Hwang, J.Y.,
2013. *Spin parameters of LAGEOS-1 and LAGEOS-2 spectrally determined from Satellite Laser Ranging data*. Adv. Space Res. 52, 1332–1338.



SLR, POD and Models



M. Visco, D. Lucchesi, *Comprehensive model for the spin evolution of the LAGEOS and LARES satellites*. Phys. Rev. D 98, 044034
doi:10.1103/PhysRevD.98.044034, 2018

LASSOS Spin Model: results for LAGEOS II

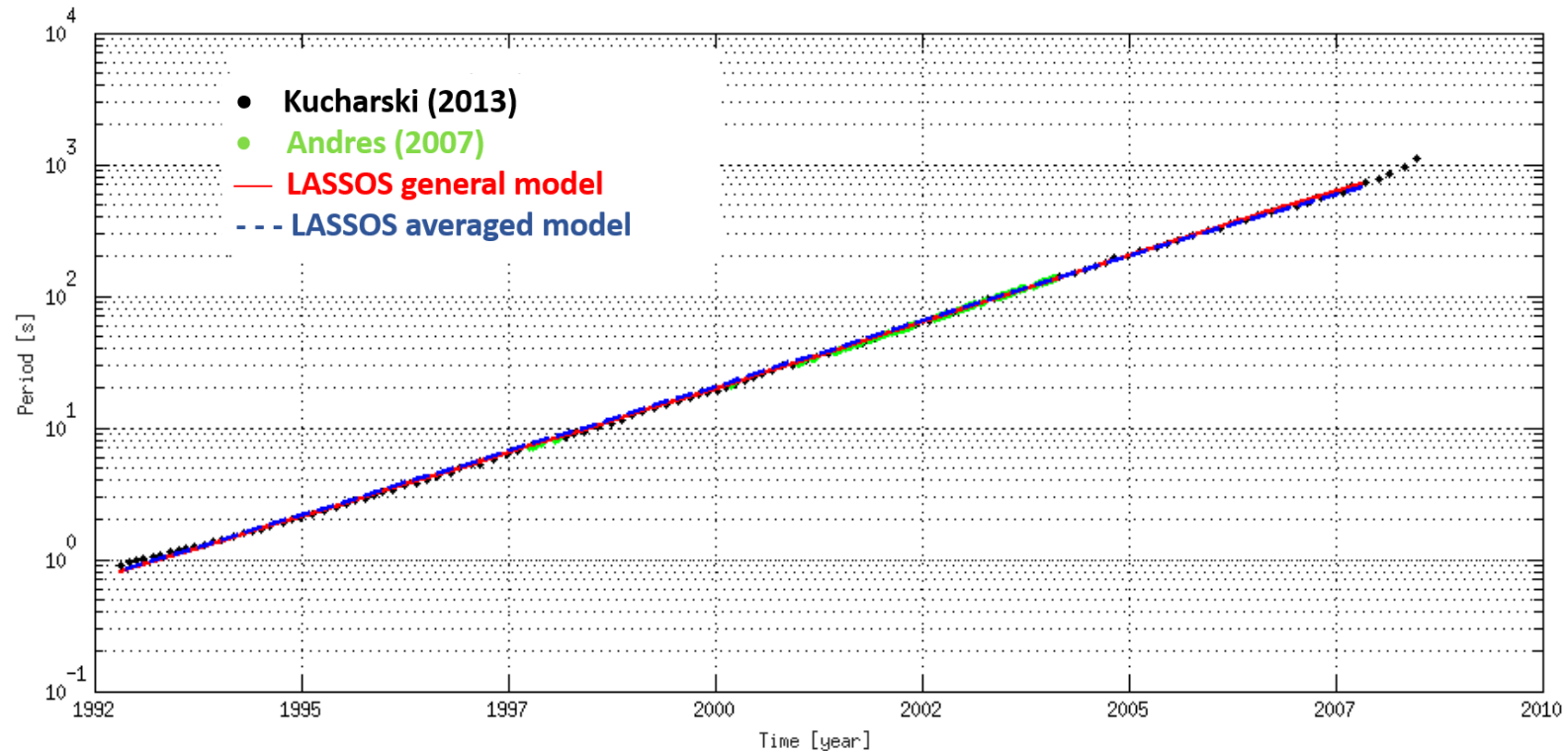
Blue = LASSOS model for the rapid-spin

Red = LASSOS general model

LArase Satellites Spin mOdel Solutions (LASSOS)

Rotational Period: P

Andrés de la Fuente, J.I.,
2007. *Enhanced Modelling of LAGEOS Non-Gravitational Perturbations* (Ph.D. thesis). Delft University Press. Sieca Repro, Turbineweg 20, 2627 BP Delft, The Netherlands.
Kucharski, D., Lim, H.C., Kirchner, G., Hwang, J.Y.,
2013. *Spin parameters of LAGEOS-1 and LAGEOS-2 spectrally determined from Satellite Laser Ranging data*. Adv. Space Res. 52, 1332–1338.



Local Lorentz Invariance

Local Lorentz Invariance (LLI) represents a pillar of the **Standard Model (SM)** of particles and fields as well as of Einstein's theory of **General Relativity (GR)**.

LLI states that the outcome of any **local** (in space and time) non-gravitational experiment is **independent** of the **velocity** of the **freely-falling** reference frame in which the experiment is performed.

Modern unification theories suggest that the gravitational long-range interaction between macroscopic bodies may be mediated, not only by the metric tensor field $g_{\mu\nu}$ of **GR** but also by other fields, as **scalar**, **vector**, or **tensor** fields.

More generally, besides **GR**, any metrically coupled **tensor-scalar** theory of gravitation does not predict **any violation** of **local boost invariance**. This is for example the case of the **Brans-Dicke** theory of gravitation which predicts the existence of a scalar field ϕ .

However, in the case of theories that contain **vector fields** or other **tensor fields**, in addition to the metric tensor $g_{\mu\nu}$, one expects that the **global distribution of matter** in the **Universe** to select a preferred rest frame for the local gravitational interaction.

In this case the **physical laws** could be **different** from a **moving observer** with respect to a **stationary one**, as well as from the orientation...

Local Lorentz Invariance

In theories of gravity with $\begin{cases} g_{\mu\nu} \\ \phi \end{cases}$ LLI holds, while in theories with $\begin{cases} g_{\mu\nu} \\ K^\mu \end{cases}$ or with $\begin{cases} g_{\mu\nu} \\ C_{\mu\nu} \end{cases}$ LLI is violated.

From the phenomenological point of view, and in the framework of the **Parametrized-Post Newtonian (PPN)** formalism [1,2,3], valid in the **weak-field** and **slow-motion (WFSM)** limit of **GR**, the **Preferred Frame Effects (PFE)** are described by the parameters **α_1** , **α_2** and **α_3** , all equal to zero in **GR** and in tensor-scalar theories of gravity.

In particular, in the case of the interaction of **N** ideal test masses, the **Lagrangian** depends on the two parameters **α_1** and **α_2** , that, if different from zero, will provide non-boost invariant terms depending on the **velocities** (v_a^0) of the test masses with respect to some **gravitationally preferred rest frame** [4]:

$$\mathcal{L}^N = \mathcal{L}_{\beta,\gamma,\eta} + \mathcal{L}_{\alpha_1} + \mathcal{L}_{\alpha_2}$$

$$\mathcal{L}_{\alpha_1} = -\frac{\alpha_1}{4c^2} \sum_{a \neq b} \frac{Gm_a m_b}{r_{ab}} (\mathbf{v}_a^0 \cdot \mathbf{v}_b^0)$$

1. Nordtvedt, K. *Equivalence Principle for Massive Bodies. II. Theory*. Phys. Rev. **1968**, 169, 1017–1025

2. Will, C.M. *Theoretical Frameworks for Testing Relativistic Gravity. II. Parametrized Post-Newtonian Hydrodynamics, and the Nordtvedt Effect*. Astrophys. J. **1971**, 163, 611–628

3. Will, C.M.; Nordtvedt, K. *Conservation Laws and Preferred Frames in Relativistic Gravity. I. Preferred-Frame Theories and an Extended PPN Formalism*. Astrophys. J. **1972**, 177, 757–774

4. Damour, T.; Esposito-Farese, G. *Testing for preferred-frame effects in gravity with artificial Earth satellites*. Phys. Rev. D **1994**, 49, 4, 1693-1706

Local Lorentz Invariance

Local Lorentz Invariance is a key ingredient of the Equivalence Principle.

Einstein Equivalence Principle (EEP)

valid in **GR** and in all **metric theories** of gravity:

1. WEP
2. LLI
3. LPI

Strong Equivalence Principle (SEP)

valid in **GR**:

1. GWEP
2. LLI
3. LPI

GWEP = Gravitational Weak Equivalence Principle. It means that **WEP** is valid for **self-gravitating bodies** as well as for test bodies.

$$\mathcal{L}^N = \mathcal{L}_{\beta, \gamma, \eta} + \mathcal{L}_{\alpha_1} + \mathcal{L}_{\alpha_2}$$

Nordtvedt effect

$$G_{ab} = G \left[1 + \eta \left(\frac{E_a^{grav}}{m_a c^2} + \frac{E_b^{grav}}{m_b c^2} \right) \right]$$

$$\eta = 4\beta - \gamma - 3 - \alpha_1 + \frac{2}{3}\alpha_2$$

$$\begin{aligned} \beta &= \gamma = 1 \\ \alpha_1 &= \alpha_2 = 0 \end{aligned}$$

in **GR**

Local Lorentz Invariance

LLI and, consequently, PFE, are **well tested** in the context of **high-energy physics experiments** but are **much more difficult** to test in the context of **gravitation**, both in the **weak-field** regime and in the **strong- or quasi-strong-field** regime.

Living Rev. Relativity, 8, (2005), 5
<http://www.livingreviews.org/lrr-2005-5>

Modern Tests of Lorentz Invariance

David Mattingly
Department of Physics
University of California at Davis
Davis, CA 95616, U.S.A.
email: mattingly@physics.ucdavis.edu
<http://lifshitz.ucdavis.edu/~mattingly>

Accepted on 4 July 2005
Published on 7 September 2005

Living Reviews in Relativity

Published by the
Max Planck Institute for Gravitational Physics
(Albert Einstein Institute)
Am Mühlenberg 1, 14424 Golm, Germany
ISSN 1433-8351

Abstract

Motivated by ideas about quantum gravity, a tremendous amount of effort over the past decade has gone into testing Lorentz invariance in various regimes. This review summarizes both the theoretical frameworks for tests of Lorentz invariance and experimental advances that have made new high precision tests possible. The current constraints on Lorentz violating effects from both terrestrial experiments and astrophysical observations are presented.

IOP PUBLISHING

CLASSICAL AND QUANTUM GRAVITY

Class. Quantum Grav. 30 (2013) 133001 (50pp)

[doi:10.1088/0264-9381/30/13/133001](https://doi.org/10.1088/0264-9381/30/13/133001)

TOPICAL REVIEW

Tests of Lorentz invariance: a 2013 update

S Liberati

SISSA, Via Bonomea 265, I-34136 Trieste, Italy
INFN, Via Valerio 2, I-34100 Trieste, Italy

E-mail: liberati@sissa.it

Received 28 February 2013, in final form 22 March 2013

Published 7 June 2013

Online at stacks.iop.org/CQG/30/133001

Abstract

We present an updated review of Lorentz invariance tests in effective field theories (EFTs) in the matter as well as in the gravity sector. After a general discussion of the role of Lorentz invariance and a derivation of its transformations along the so-called von Ignatovski theorem, we present the dynamical frameworks developed within local EFT and the available constraints on the parameters governing the Lorentz breaking effects. In the end, we discuss two specific examples: the OPERA ‘affaire’ and the case of Hořava–Lifshitz gravity. The first case will serve as an example, and a caveat, of the practical application of the general techniques developed for constraining Lorentz invariance violation to a direct observation potentially showing these effects. The second case will show how the application of the same techniques to a specific quantum gravity scenario has far-reaching implications not foreseeable in a purely phenomenological EFT approach.

PACS numbers: 98.70.Rz, 04.60.–m, 11.30.Cp, 12.20.Fv

Local Lorentz Invariance



In 1994, **Damour** and **Esposito-Farese** have shown that the orbits of some **artificial satellites** have the potential to provide improvements in the **limit** of the α_1 parameter down to the 10^{-6} level, thanks to the appearance of **small divisors** which enhance the corresponding **PFE**.

PHYSICAL REVIEW D

VOLUME 49, NUMBER 4

15 FEBRUARY 1994

ARTICLES

Testing for preferred-frame effects in gravity with artificial Earth satellites

Thibault Damour

*Institut des Hautes Etudes Scientifiques, 91440 Bures sur Yvette, France
and Département d'Astrophysique Relativiste et de Cosmologie, Observatoire de Paris,
Centre National de la Recherche Scientifique, 92195 Meudon, France*

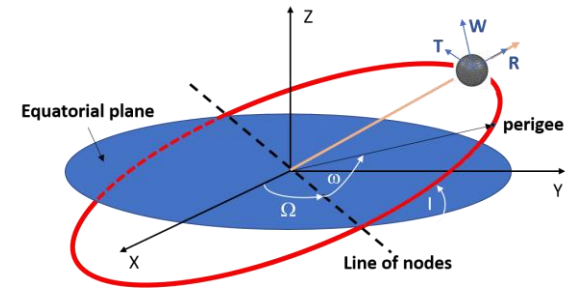
Gilles Esposito-Farèse

*Centre de Physique Théorique, Centre National de la Recherche Scientifique,
Luminy, Case 907, 13288 Marseille Cedex 9, France*

(Received 8 October 1993)

As gravity is a long-range force, one might *a priori* expect the Universe's global matter distribution to select a preferred rest frame for local gravitational physics. At the post-Newtonian approximation, two parameters suffice to describe the phenomenology of preferred-frame effects. One of them has already been very tightly constrained ($|\alpha_2| < 4 \times 10^{-7}$, 90% C.L.), but the present bound on the other one is much weaker ($|\alpha_1| < 5 \times 10^{-4}$, 90% C.L.). It is pointed out that the observation of particular orbits of artificial Earth satellites has the potential of improving the α_1 limits by a couple of orders of magnitude, thanks to the appearance of small divisors which enhance the corresponding preferred-frame effects. There is a discrete set of inclinations which lead to arbitrarily small divisors, while, among zero-inclination (equatorial) orbits, geostationary ones are near optimal. The main α_1 -induced effects are (i) a complex secular evolution of the eccentricity vector of the orbit, describable as the vectorial sum of several independent rotations, and (ii) a yearly oscillation in the longitude of the satellite.

Local Lorentz Invariance



In our analysis:

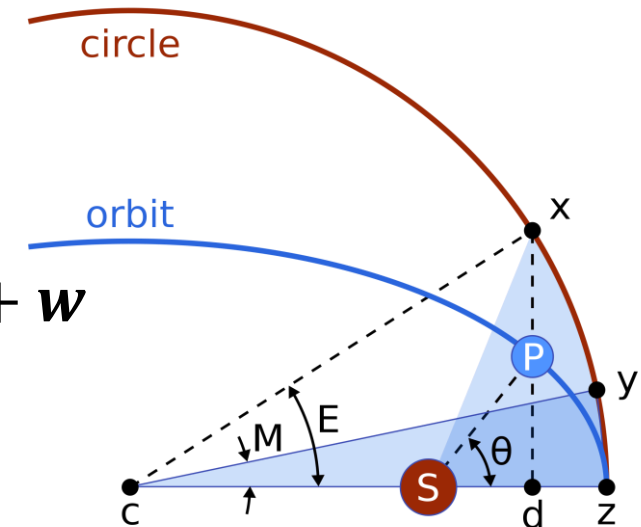
- we concentrated upon the **yearly oscillation** of the **longitude** ($\omega + M$) of the **LAGEOS II** satellite
- as **gravitationally preferred rest frame** we consider that of the **cosmic background radiation**
- **w** represents the speed of the **Sun** with respect to this reference frame with orientation given by the following ecliptic coordinates (λ_{PF}, β_{PF}):

$$w = 368 \pm 2 \frac{km}{s} \quad \begin{cases} \lambda_{PF} = 171^\circ.55 \\ \beta_{PF} = -11^\circ.13 \end{cases}$$

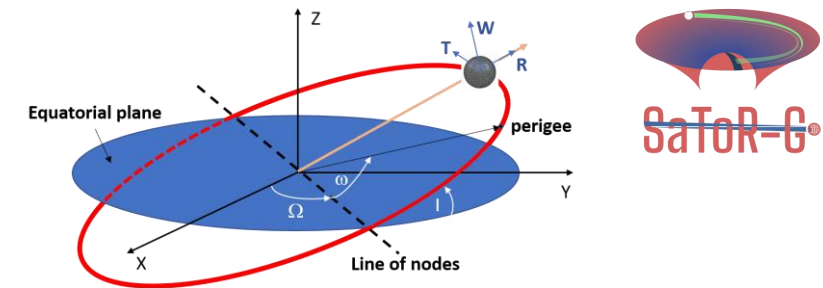
$$\mathcal{L}_{\alpha_1} = -\frac{\alpha_1}{4c^2} \sum_{a \neq b} \frac{Gm_a m_b}{r_{ab}} (\mathbf{v}_a^0 \cdot \mathbf{v}_b^0)$$

$$\mathbf{v}_s^0 = \mathbf{v}_s + \mathbf{v}_\oplus + \mathbf{w}$$

$$\mathcal{L}_{\alpha_1} = -\frac{\alpha_1}{2c^2} \frac{GM_\oplus m_s}{r_{\oplus s}} (\mathbf{v}_\oplus + \mathbf{w}) \cdot (\mathbf{v}_s + \mathbf{v}_\oplus + \mathbf{w})$$



Local Lorentz Invariance



From **Lagrange's perturbative equations** we are able to extract the perturbative effect of a possible **PFE** on the **rate** of the **argument of pericenter** and on the **rate of the mean anomaly** of the satellite.

$$\frac{d\omega}{dt} = \frac{\sqrt{1-e^2}}{na^2e} \frac{\partial R}{\partial e} - \frac{\cot i}{na^2\sqrt{1-e^2}} \frac{\partial R}{\partial i}$$

$$\frac{dM}{dt} = -\frac{2}{na} \frac{\partial R}{\partial a} - \frac{1-e^2}{na^2e} \frac{\partial R}{\partial e}$$

R represents the perturbing function
 $(a, e, i, \Omega, \omega, M)$ are the keplerian elements
 n represents the satellite mean motion: $n = \sqrt{\frac{GM_{\oplus}}{a^3}}$

We finally obtain:

$$(\dot{\omega} + \dot{M})_{\alpha_1} = -\alpha_1 2n \frac{wv_{\oplus}}{c^2} \cos \beta_{PF} \sin(n_{\oplus}t - \lambda_{PF}) + \dots$$

If **PFEs** exist, the quantity $(\dot{\omega} + \dot{M})_{\alpha_1}$ must be present in the **residuals** of the two elements obtained from the satellite **POD**.

Local Lorentz Invariance



POD of the LAGEOS II satellite

- **GEODYN II s/w**

- Timespan of 10311 days (about 28.3 years)
- Arc length: 7 days
- General Relativity: not modeled
- Empirical accelerations, CR, ...: not estimated
- Non-gravitational perturbations: internal and external
- Gravity field: from GRACE solutions
- State-vector adjusted to best fit the tracking data
- ...

Local Lorentz Invariance

Procedure in the time domain to extract the constraint in the PPN parameter α_1 .

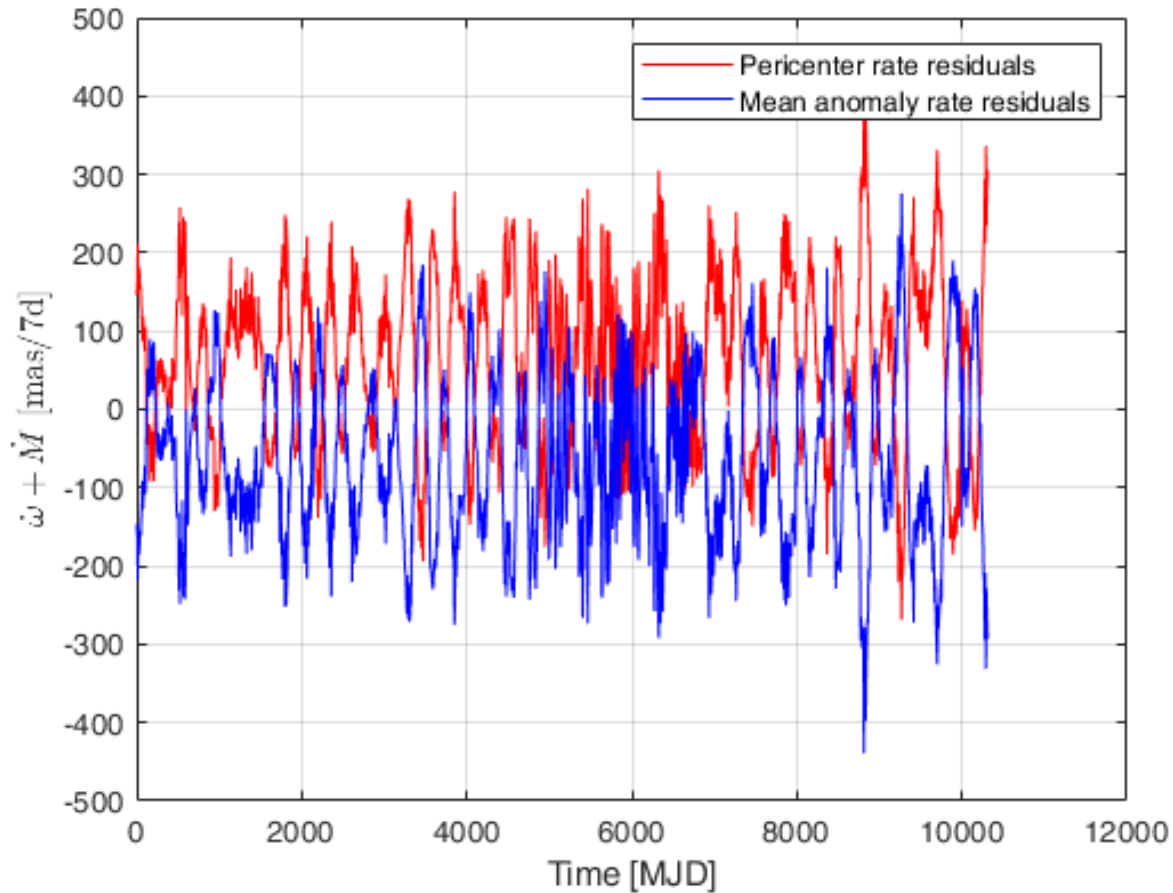
1. From the **POD** we estimated the satellite **state-vector** for each **arc**
2. From the **state-vectors** we obtain the **residuals** in the **rate** of the orbital elements: $\dot{\omega}$ and \dot{M}
3. From these **residuals** we build our **gravitational observable**: $\dot{\omega} + \dot{M}$
4. We remove from the **observable** the **predictions** of the **unmodeled relativistic precessions** of **GR**
5. We **Pass-Band filter** this new (corrected) observable around the **yearly frequency**
6. We apply a **Lock-in** to these data at the **expected frequency (the annual one)** for the effect described by the α_1 parameter and linked to the existence of the **PFE** due to the **cosmic background radiation**
7. We calculate the **mean** from this last operation and from this **mean**, suitably renormalized, we **extract** the value of the **PPN** parameter α_1 .

$$(\dot{\omega} + \dot{M})_{\alpha_1} = -\alpha_1 2n \frac{wv_{\oplus}}{c^2} \cos \beta_{PF} \sin(n_{\oplus}t - \lambda_{PF}) + \dots = \alpha_1 K \sin(n_{\oplus}t - \lambda_{PF}) + \dots$$

$$K = -2n \frac{wv_{\oplus}}{c^2} \cos \beta_{PF}$$

Local Lorentz Invariance

Residuals in the two observables after the POD



Relativistic precessions in the two observables

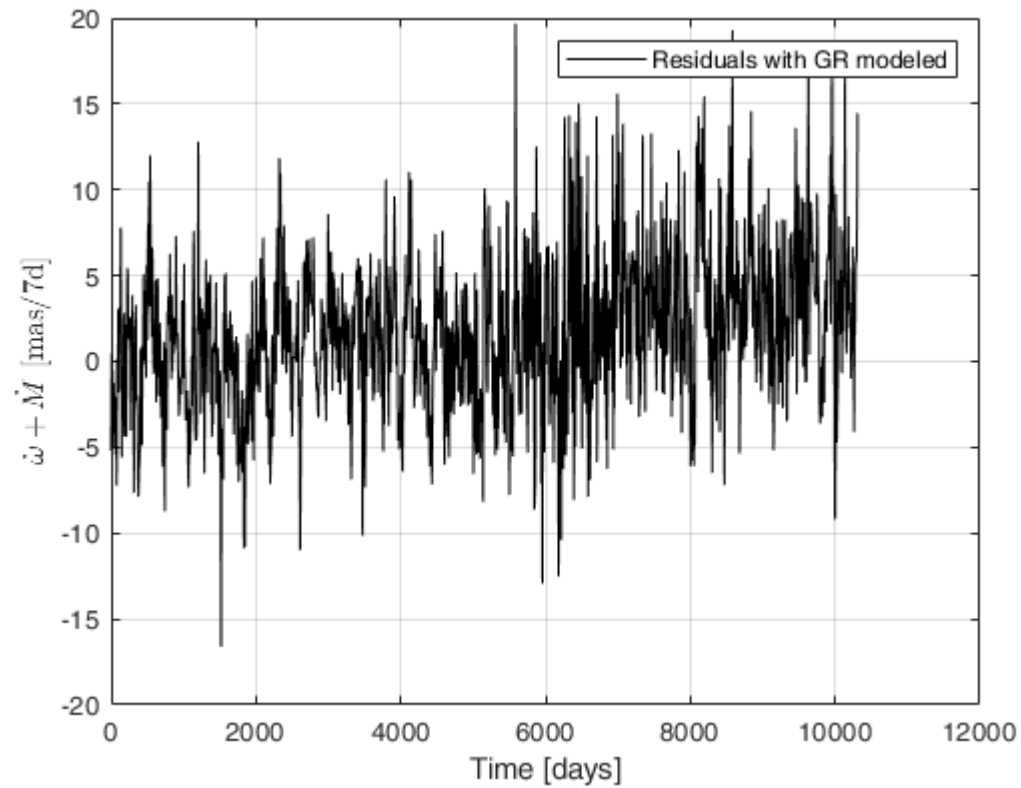
Rate (mas/yr)	LAGEOS	LAGEOS II	LARES
$\dot{\omega}_{Schw}$	+ 3270.78	+ 3352.58	+ 10,110.15
$\dot{\omega}_{LT}$	+ 31.23	- 57.33	- 124.53
$\dot{\omega}_{J_2}^{dir}$	- 3.26	+ 2.85	- 23.38
$\dot{\omega}_{J_2}^{indir}$	- 0.36	+ 0.16	- 2.65
Total	+ 3306.38	+ 3298.26	+ 9959.59
\dot{M}_{Schw}	- 3278.75	- 3352.26	- 10,110.14
\dot{M}_{J_2rel}	- 0.92	+ 0.15	- 6.71
Total	- 3278.75	- 3352.11	- 10,116.85

$$\frac{d\omega}{dt} = \frac{\sqrt{1-e^2}}{na^2e} \frac{\partial R}{\partial e} - \frac{\cot i}{na^2\sqrt{1-e^2}} \frac{\partial R}{\partial i}$$

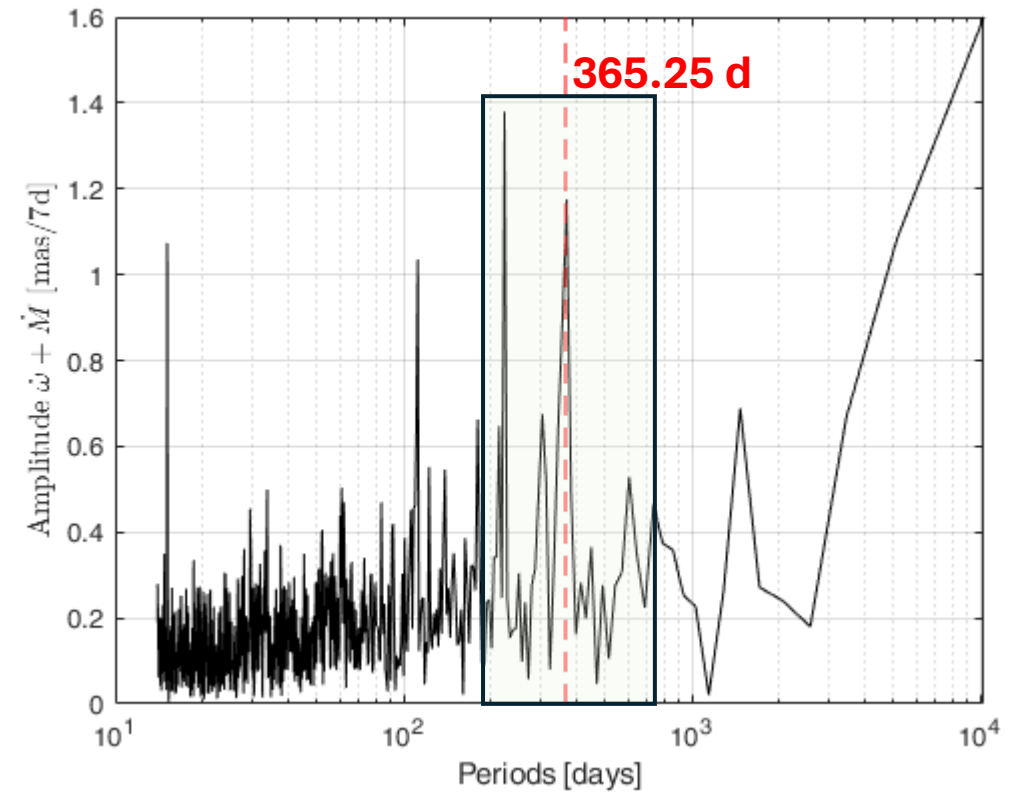
$$\frac{dM}{dt} = -\frac{2}{na} \frac{\partial R}{\partial a} - \frac{1-e^2}{na^2e} \frac{\partial R}{\partial e}$$

Local Lorentz Invariance

Residuals in the observable $\dot{\omega} + \dot{M}$

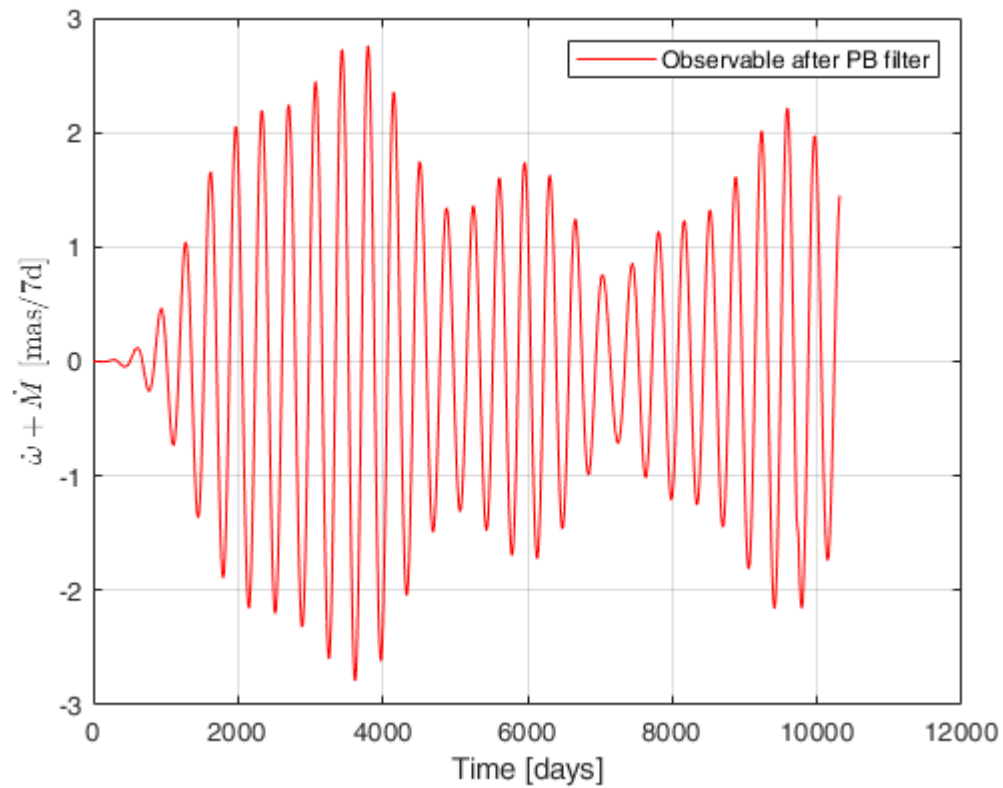


FFT of the Residuals in the observable

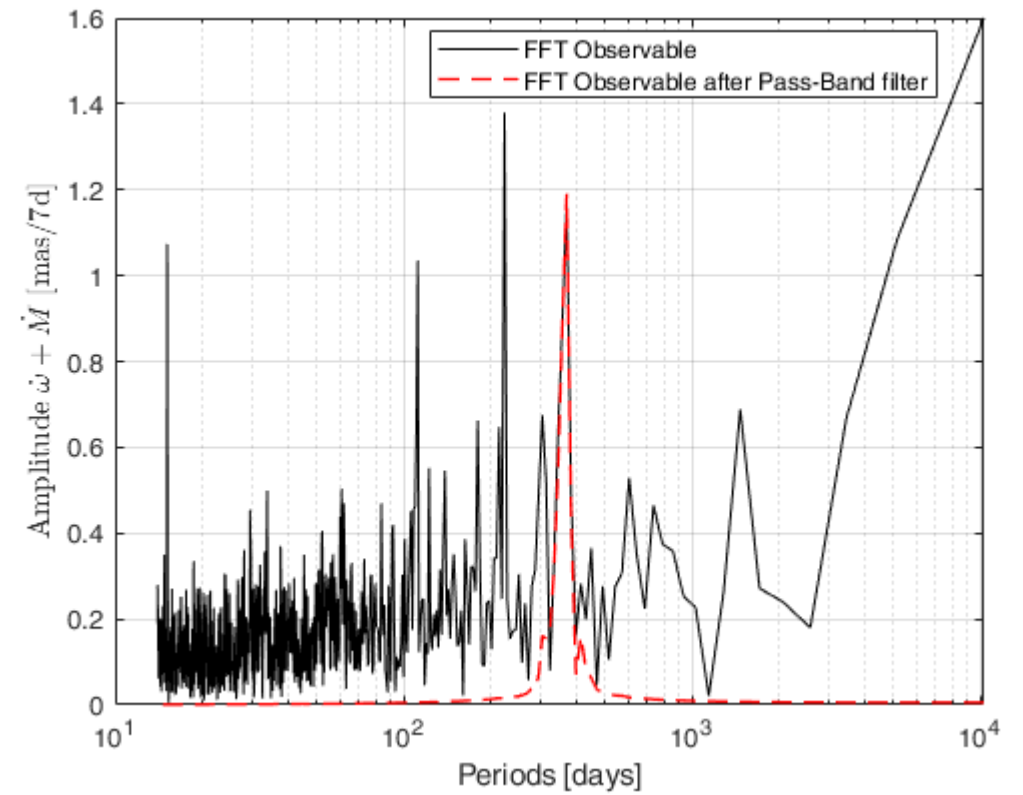


Local Lorentz Invariance

Residuals in the observable after Pass-Band filtering



FFT of the Residuals in the observable



Local Lorentz Invariance

Lock-in analysis

$$(\dot{\omega} + \dot{M})_{\alpha_1} = \alpha_1 K \sin(n_{\oplus} t - \lambda_{PF}) + \dots \quad K = -2n \frac{wv_{\oplus}}{c^2} \cos \beta_{PF}$$

$$\sin(n_{\oplus} t - \lambda_{PF}) \cdot (\dot{\omega} + \dot{M})_{res} = \alpha_1 K (\sin(n_{\oplus} t - \lambda_{PF}))^2 + \dots$$

Lock-in analysis, in this case more properly a **homodyne analysis (phase sensitive detection)**, is mathematically based on **Werner's trigonometric formulas**:

$$\sin \alpha \sin \beta = \frac{1}{2} (\cos(\alpha - \beta) - \cos(\alpha + \beta))$$

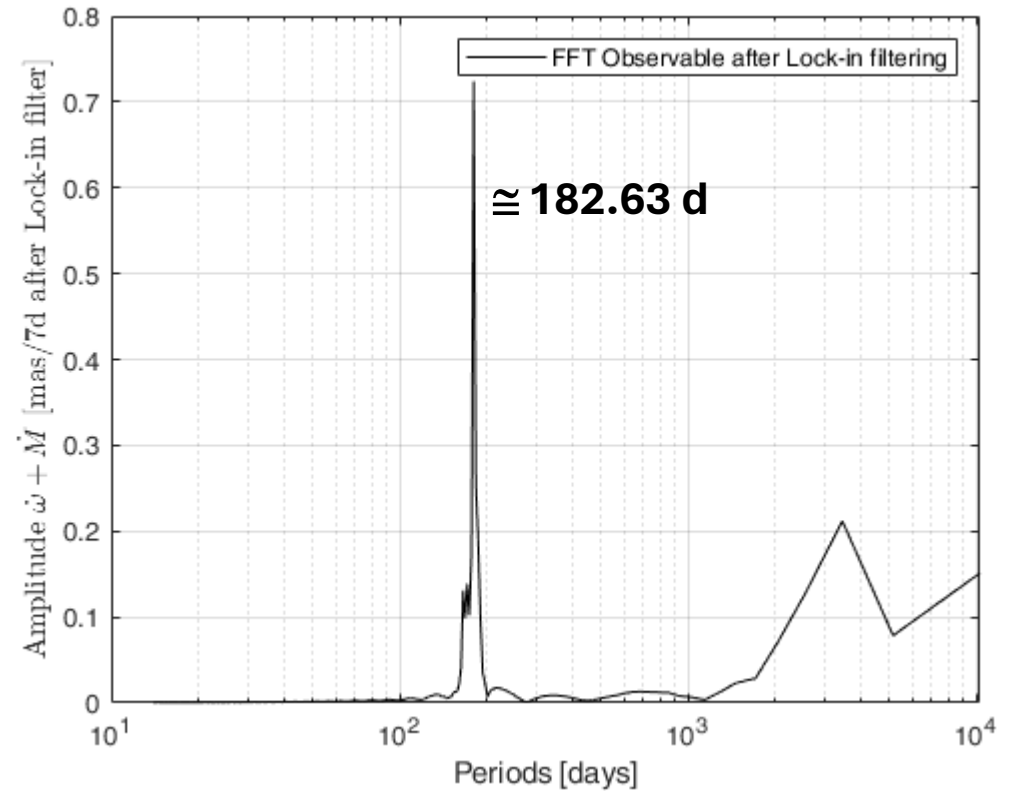
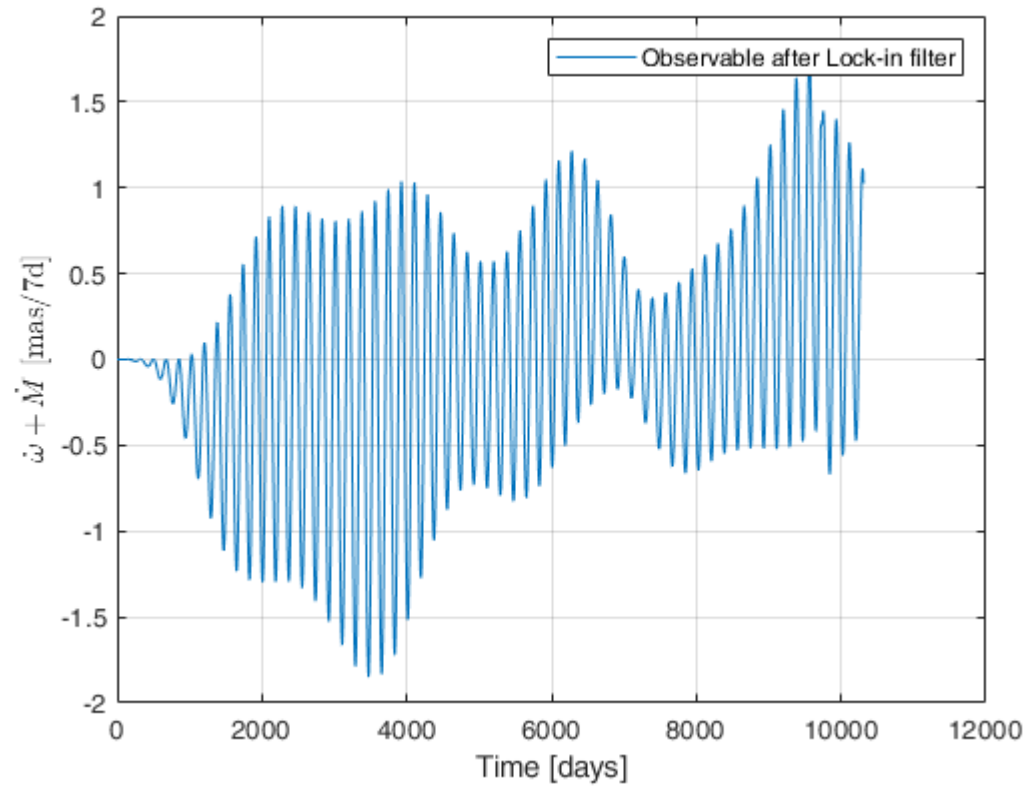
$$\sin \alpha \cos \beta = \frac{1}{2} (\sin(\alpha - \beta) + \sin(\alpha + \beta))$$

$$\sin \alpha \sin \alpha = \frac{1}{2} (1 - \cos(2\alpha))$$

If $\alpha = \beta$, as in our case, a **part of the signal** goes in **continuous (DC)** and a **part at twice the annual frequency**.

Local Lorentz Invariance

Lock-in analysis



$$\alpha_1 = \left\langle (\dot{\omega} + \dot{M})_{res} \right\rangle \frac{2}{K}$$

Local Lorentz Invariance



Preliminary result for the **PPN** parameter α_1 and constraints to alternative theories of gravitation:

$$\alpha_1 = +1.57 \times 10^{-6}$$

1. This result represents the **first constraint in α_1** in the **field** of the **Earth** based on a **pure gravitational experiment**.
2. The result obtained, although preliminary, confirms the validity of the **LLI** for gravity and strongly constrains possible **PFEs** and, consequently, **vector-tensor theories of gravity**, at least in the **WFSM** limit of **GR: Einstein-~~Æ~~ther theory**.

Local Lorentz Invariance

Preliminary result for the **PPN** parameter α_1 and constraints to alternative theories of gravitation:

$$\alpha_1 = +1.57 \times 10^{-6}$$

1. This result represents the **first constraint in α_1** in the **field** of the **Earth** based on a **pure gravitational experiment**.
2. The result obtained, although preliminary, confirms the validity of the **LLI** for gravity and strongly constrains possible **PFEs** and, consequently, **vector-tensor theories of gravity**, at least in the **WFSM** limit of **GR: Einstein-Æther theory**.
3. We have also performed a **sensitivity analysis** on the **value** of the **PPN parameter α_1** by constructing a **distribution** of its values as **the Lock-in frequency** and signal **phase** vary **randomly** on a sample of **10^5 values** each. We consequently obtained a **two-parameter distribution** of α_1 for evaluating the possible violation signal of **GR**.

Results from the sensitivity analysis:

$$\langle \alpha_1 \rangle = 1.4 \times 10^{-7}$$

$$\text{rms}(\alpha_1) = \sigma(\alpha_1) \cong 6.850 \times 10^{-5}$$

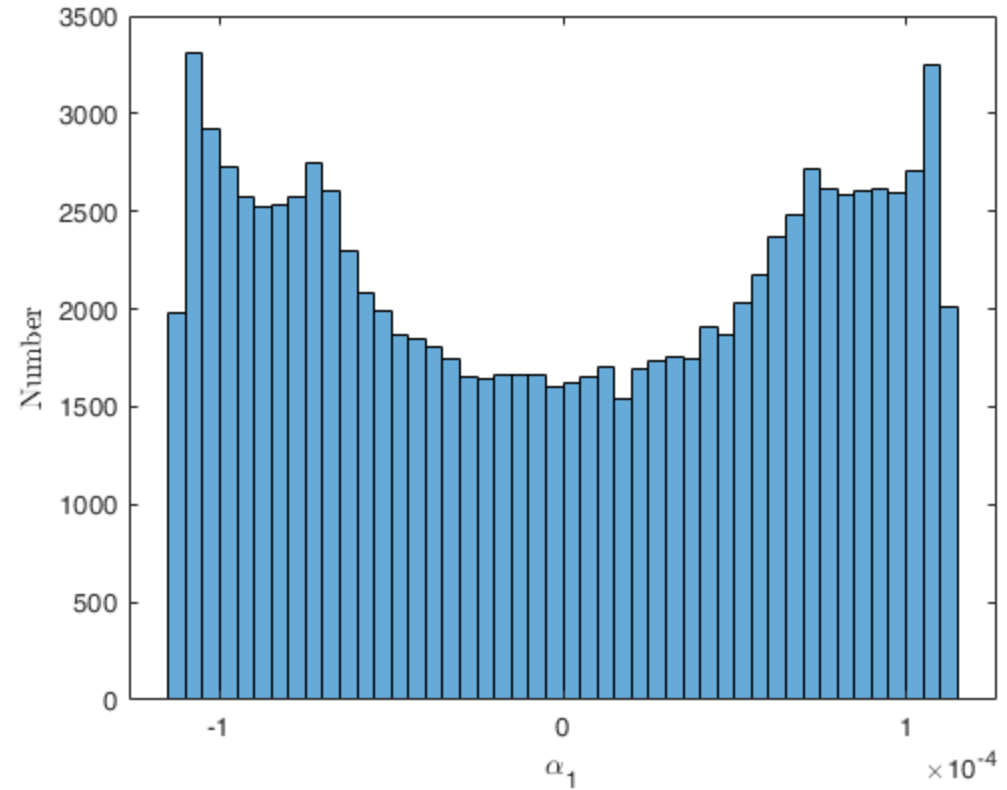
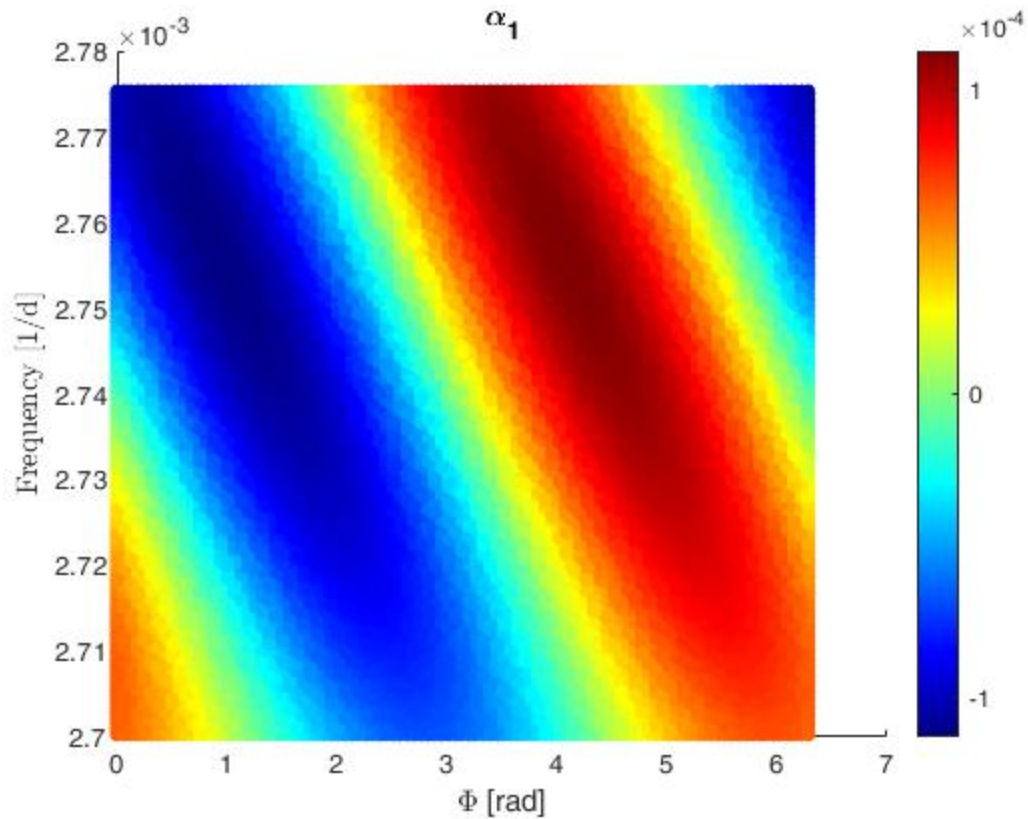
$$\max(\alpha_1) = +1.1283 \times 10^{-4}$$

$$\text{median}(\alpha_1) = 1.5 \times 10^{-7}$$

$$\min(\alpha_1) = -1.1283 \times 10^{-4}$$

Local Lorentz Invariance

Sensitivity analysis:



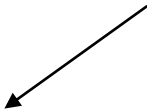
Local Lorentz Invariance

Preliminary **error budget** for the **systematic errors**:


<ol style="list-style-type: none"> 1. Gravitational field (quadrupole) 2. Solid tides 3. Ocean tides 4. Non-Gravitational Perturbations: 	$\delta\alpha_1 \cong 1.6 \times 10^{-5}$ $\delta\alpha_1 < 9 \times 10^{-10}$ $\delta\alpha_1 \lesssim 2 \times 10^{-7}$ $\delta\alpha_1 \cong 0$	$\left. \vphantom{\begin{matrix} \delta\alpha_1 \cong 1.6 \times 10^{-5} \\ \delta\alpha_1 < 9 \times 10^{-10} \\ \delta\alpha_1 \lesssim 2 \times 10^{-7} \\ \delta\alpha_1 \cong 0 \end{matrix}} \right\} \delta\alpha_1 \cong 1.6 \times 10^{-5}$
--	---	--

Very preliminary evaluation of the measure on the constraint to the parameter **α_1** :

$$\alpha_1 = +1.6 \times 10^{-6} \pm 7 \times 10^{-5}$$



From the measure



From the distribution

Local Lorentz Invariance



Comparison with the literature:

$$\alpha_1 = +1.6 \times 10^{-6} \pm 7 \times 10^{-5}$$

With **SLR** data from **LAGEOS II longitude**, 2023

$$\alpha_1 = -7 \times 10^{-5} \pm 9 \times 10^{-5}$$

With **LLR** data from the **oscillations** of the **Earth-Moon distance**, 2008

$$\hat{\alpha}_1 = -4 \times 10^{-6} \pm 4 \times 10^{-5}$$

From **binary Pulsar** data, 2012

Müller J, Williams J G and Turyshev S G, 2008. Lunar laser ranging contributions to relativity and geodesy. *Lasers, Clocks and Drag-Free Control: Exploration of Relativistic Gravity in Space (Astrophysics and Space Science Library vol 349)* ed H Dittus, C Lammerzahn and S G Turyshev p 457.

J. Müller, K. Nordtvedt, D. Vokrouhlický, *Improved constraint on the α_1 PPN parameter from lunar motion*. Phys. Rev. D, Vol. 54, No 10, 1996.

L. Shao, N. Wex, *New tests of Local Lorentz invariance of gravity with small-eccentricity binary pulsars*. Class. Quantum Grav. 29, 2012.

Conclusions

- **Local Lorentz Invariance** represents one of the cornerstones of both the standard model (SM) of field and particle physics and the standard model of gravitation, i.e. of **GR**. In a sense, **LLI** represents our current deepest understanding of the nature of space and time. So, why test **LLI**?
- A strong motivation in our work is to search for the possible existence (or at least evidence) of **new physics** beyond **GR**. We mentioned the possible existence of additional fields that come into play in mediating the gravitational interaction and that could couple to matter in such a way, in some cases, that they violate Lorentz invariance.
- Therefore, in this work we have presented and discussed a test of **LLI**, and its possible violation, in the gravitational sector by exploiting the possible existence of **PFE**.

$$\alpha_1 = +1.6 \times 10^{-6} \pm 7 \times 10^{-5}$$

- The result we have obtained further constrains the possible existence of a preferred frame for local gravitational physics and, consequently, that of theories of gravitation described, in addition to the **metric tensor** of **GR**, by the presence of additional fields of **tensor** and/or **vector** nature, such as for example the case of **Einstein-aether** theory, i.e. of **vector-tensor theories** of gravitation.
- Consequently, this new result represents a first constraint on **LLI** through a **weak-field gravity experiment** with a satellite orbiting the Earth.

The SaToR-G Team



@IAPS-INAFA, Tor Vergata (RM)

Marco Cinelli
Alessandro Di Marco
David Lucchesi
Marco Lucente
Carmelo Magnafico
Roberto Peron
Feliciano Sapiro
Massimo Visco



@Dept. Physics, Univ. Tor Vergata (RM)

Massimo Bassan
Giuseppe Pucacco



@ISTI-CNR, Pisa

Luciano Anselmo
Carmen Pardini



@IGN, Yebes (Spain)

José Carlos Rodríguez

